

# OGLE-II High Proper Motion Stars towards the Galactic centre

Nicholas J. Rattenbury<sup>1</sup> and Shude Mao<sup>1\*</sup>

<sup>1</sup> Jodrell Bank Centre for Astrophysics, Alan Turing Building, The University of Manchester, Manchester, M13 9PL, UK

Accepted ..... Received .....; in original form .....

## ABSTRACT

The photometry data base of the second phase of the OGLE microlensing experiment, OGLE-II, is a rich source of information about the kinematics and structure of the Galaxy. In this work we use the OGLE-II proper motion catalogue to identify candidate stars which have high proper motions. 521 stars with proper motion  $\mu > 50 \text{ mas yr}^{-1}$  in the OGLE-II proper motion catalogue (Sumi et al. 2004) were cross-identified with stars in the MACHO high proper motion catalogue, and the DENIS and 2MASS infra-red photometry catalogues. Photometric distances were computed for stars with colours consistent with G/K and M type stars. 6 stars were newly identified as possible nearby ( $< 50 \text{ pc}$ ) M dwarfs.

**Key words:** Stars: statistics - Stars: distances - solar neighbourhood

## 1 INTRODUCTION

Several microlensing collaborations have carried out survey observations of many square degrees towards the Galactic centre, including the EROS (Aubourg et al. 1993), MACHO (Alcock et al. 2000), MOA (Bond et al. 2001; Sumi et al. 2003a) and OGLE (Udalski et al. 2000) groups. As a result of these extended survey campaigns, large data bases were generated, containing the photometry of millions of stars in and towards the Galactic centre. These data bases can be used to investigate the structure, kinematics and stellar populations of the central regions of the Galaxy. For instance, red clump giants in the OGLE-II photometry database were used to constrain the shape and orientation of the Galactic bar (Rattenbury et al. 2007b).

Many fundamental parameters of stellar astrophysics such as mass, temperature and luminosity, are derived from the observation of stars in the solar neighbourhood. Our understanding of the nature of the Galaxy is also advanced through studies of the kinematics, chemical abundance and mass function of these nearby stars. A census of nearby stars has not been achieved however, with estimates of the sample deficit ranging from  $\sim 25\%$  of stars within  $10 \text{ pc}$  (Reid et al. 2003) to  $\gtrsim 30\%$  (Henry et al. 1997).

We select high proper motion stars from the OGLE-II proper motion data base (Sumi et al. 2004) and cross-identify them with known high proper motion stars from the MACHO high proper motion catalogue (Alcock et al. 2001). We obtain photometric distance estimates for OGLE-II high

proper motion stars which have corresponding entries in the *DEep Near-Infrared Survey* of the southern sky (DENIS) (Epchtein et al. 1997; The Denis Consortium 2005). In Section 2 we describe the OGLE-II proper motion data base and in Section 3 we describe how the high proper motion candidate stars were selected. Section 4 describes how the cross-identification was made between the OGLE-II high proper motion star candidates and entries in the DENIS data base. In Section 5 we produce photometric distance estimates for OGLE-II stars cross-identified with DENIS stars. Stars with photometric distances  $< 50 \text{ pc}$  are cross-identified with entries in the *Two-Micron All Sky Survey* (2MASS) catalogue and compared to a set of known cool dwarfs in Section 6. Section 7 contains a discussion on our results.

## 2 OGLE-II PROPER MOTION CATALOGUE

During the second phase of the OGLE experiment (OGLE-II), between 1997 and 2000, the Galactic centre was observed in 49 fields using the 1.3m Warsaw telescope at the Las Campanas Observatory, Chile. Each field was  $0.24^\circ \times 0.95^\circ$  in size, the median seeing over the almost 4 year baseline was  $\sim 1.3 \text{ arcsec}$ . The OGLE-II fields extend across the central regions of the Galactic bulge with  $-11^\circ < l < +11^\circ$  and  $-6^\circ < b < +3^\circ$ , see Figure 2. Further details of the telescope, camera and operations can be found in Udalski et al. (1997).

Sumi et al. (2004) determined the proper motions for millions of stars in the OGLE-II fields. The catalogue contains proper motion data for all stars with magnitudes in

\* e-mail: (nicholas.rattenbury,shude.mao)@manchester.ac.uk

the range  $11 \leq I \leq 18$ , and includes proper motions up to  $\mu = 500 \text{ mas yr}^{-1}$ , with an accuracy of better than  $1 \text{ mas yr}^{-1}$  for stars with  $12 < I < 14$ .

The catalogue of proper motions of stars in the OGLE-II fields (Sumi et al. 2004) extended the work of Sumi et al. (2003b) where the streaming motion of stars around the Galactic bar was observed using OGLE-II proper motions in one field, as predicted by Mao and Paczyński (2002). Other work which uses the full proper motion catalogue includes the comparison of proper motion dispersions to model predictions (Rattenbury et al. 2007a).

### 3 HIGH PROPER MOTION (HPM) SAMPLE

Candidate high proper motion stars are selected using the following criteria:

$$\mu > 50 \text{ mas yr}^{-1} \quad \sigma_\mu / \mu < 0.1$$

where  $\mu$  and  $\sigma_\mu$  are the star proper motion and error, respectively. Out of a total of 5080236 stars in the OGLE-II proper motion catalogue, 18907 have proper motion  $\mu > 50 \text{ mas yr}^{-1}$ . Approximately 5% of stars have  $\sigma_\mu / \mu < 0.1$ . 521 stars satisfy both the above criteria and form the set of high proper motion candidates for this work. A proper motion of  $50 \text{ mas yr}^{-1}$  at 100 pc corresponds to  $\simeq 24 \text{ km s}^{-1}$ .

#### 3.1 Cross-identification with MACHO HPM stars

Alcock et al. (2001) report 88 high proper motion stars in the MACHO Galactic bulge fields. 9 MACHO high proper motion stars are located within the OGLE-II fields. For each of these 9 stars, the nearest OGLE-II star is identified, see Table 1. There is reasonable agreement between the MACHO and OGLE-II proper motion data, see Figure 1: all are within  $2\sigma$  of each other, except for one star. Figure 2 shows the MACHO and OGLE-II fields, along with the 88 MACHO high proper motion stars and the sample of OGLE-II high proper motion star candidates.

#### 3.2 Reduced proper motion

We compute the reduced proper motion

$$H_I = I + 5 \log \mu + 5$$

where  $\mu$  is the proper motion in  $\text{arcsec yr}^{-1}$  and  $I$  is the OGLE-II  $I$ -band magnitude. Extinction is neglected as it is not expected to be a significant effect for the nearby stars of interest. Figure 3 shows the reduced proper motion of the high proper motion candidate stars as a function of  $(V-I)$ . For illustrative purposes, the reduced proper motion expected from a hypothetical pure hydrogen white dwarf (Bergeron et al. 1995) located at a distance of 10 pc with a proper motion of  $100 \text{ mas yr}^{-1}$  is included in Figure 3. A fainter or faster white dwarf would move the line relatively downwards. Similarly a brighter or slower white dwarf would move the line upward. Figure 3 shows that most of the stars in the OGLE-II high proper motion star sample are too red to be classified as white dwarf candidates. The bluest high proper motion stars which have colours consistent with white dwarfs are more likely to be late G-type stars, rather

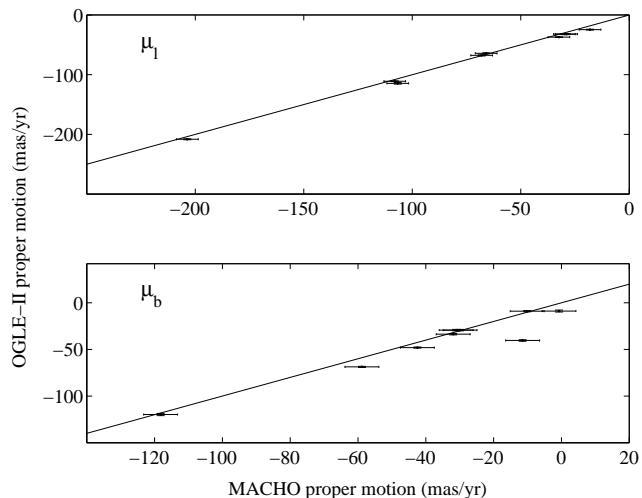


**Figure 1.** Comparison between cross-identified HPM stars in the MACHO and OGLE-II proper motion catalogues. The proper motion in the Galactic longitude and latitude directions,  $\mu_l$  (top) and  $\mu_b$  (bottom) respectively, are shown along with the line indicating  $\mu_{\text{MACHO}} = \mu_{\text{OGLE-II}}$ , see also Table 1. The MACHO proper motion accuracy is  $\sim 5 \text{ mas yr}^{-1}$  (Alcock et al. 2001); the errorbars on the OGLE-II proper motions are from the OGLE-II proper motion catalogue of Sumi et al. (2004).

than nearby ( $< 10 \text{ pc}$ ) white dwarfs (Reyl   et al. 2002). Infrared photometry is necessary in order to more accurately determine the stellar type of these high proper motion candidate stars.

The proper motion in the Galactic co-ordinate longitude and latitude directions,  $\mu_l$ ,  $\mu_b$ , respectively is shown in Figure 4 for the sample of 521 high proper motion stars. There is a clear preferred direction in the average motion of these stars. This is most likely to be due to the motion of the Sun with respect to the local standard of rest. The direction of the antapex is indicated in Figure 4, corresponding approximately with the average proper motion. This supports the theory that many of these stars are local disk objects.

#### 3.3 Parallax distance determination

The high proper motion stars are expected to display pronounced astrometric parallax signatures in their recorded position. The position of the high proper motion stars was fitted with a model similar to that of Soszynski et al. (2002) which includes parallax terms. However, as noted by Eyer and Wo  niak (2001) and Sumi et al. (2004) the influence of differential refraction is correlated with the effect of parallactic motion for stars in the Galactic bulge. A reliable parallax distance estimate for these stars was therefore not possible.

## 4 CROSS-IDENTIFICATION WITH DENIS

The OGLE-II  $I$  band filter response closely approximates the standard  $BVI$  system but diverges from standard (Landolt 1992) magnitudes for increasingly red objects (Udalski et al. 2002). For this reason we cross-correlated

**Table 1.** Cross-identified MACHO high proper motion stars from Alcock et al. (2001) with candidate stars from the OGLE-II proper motion catalogue (Sumi et al. 2004). Data from the MACHO and OGLE-II data sets are given in columns 1–5 and 6–12 respectively.  $\mu_l$  and  $\mu_b$  are the proper motions in the Galactic longitude and latitude directions respectively, measured in  $\text{mas yr}^{-1}$ . F is the OGLE-II field number.  $l$  and  $b$  are the Galactic co-ordinates of the star and  $\Delta\phi$  is the vector difference in star position between the OGLE-II and the MACHO catalogues, measured in arcsec. The accuracy of MACHO proper motions is  $\sim 5 \text{ mas yr}^{-1}$ .  $V-I$  and  $I$  denote the OGLE-II colour and magnitude of each star. The MACHO stars 101.20908.263 and 104.20908.6076 have very similar positions and proper motions and are cross-identified with only one OGLE-II star.

ID	MACHO		$\mu_l$	$\mu_b$	F	ID	OGLE-II				
	$l$ ( $^\circ$ )	$b$ ( $^\circ$ )					$\mu_l \pm \sigma_{\mu_l}$	$\mu_b \pm \sigma_{\mu_b}$	$\Delta\phi$	$V-I$	$I$
109.20894.99	2.52	-3.44	-203.64	-11.45	2	783242	$-208.2 \pm 0.8$	$-40.4 \pm 0.8$	1.00	6.19	14.49
101.21560.49	3.65	-3.22	-32.40	-42.47	18	51131	$-37.1 \pm 0.5$	$-48.0 \pm 0.6$	0.24	1.74	13.04
109.19858.98	2.51	-2.88	-108.03	-58.82	31	765538	$-111.0 \pm 0.6$	$-68.7 \pm 0.6$	0.71	2.11	13.98
114.19718.31	1.87	-3.11	-18.06	-31.92	31	240515	$-24.5 \pm 0.6$	$-33.6 \pm 0.7$	0.42	1.04	13.19
114.20882.707	1.82	-3.87	-68.01	-0.72	33	771	$-67.6 \pm 0.9$	$-8.8 \pm 1.0$	0.19	1.19	16.16
101.20908.263	3.34	-2.97	-28.88	-31.05	35	750288	$-32.0 \pm 0.8$	$-29.3 \pm 0.7$	0.41	0.86	15.14
104.20908.6076	3.34	-2.97	-29.82	-29.89	35	750288	$-32.0 \pm 0.8$	$-29.3 \pm 0.7$	0.16	0.86	15.14
101.21038.235	3.40	-3.05	-65.90	-10.09	36	426923	$-64.2 \pm 0.8$	$-8.9 \pm 0.7$	0.40	2.37	14.60
119.20607.34	0.89	-4.25	-106.67	-118.20	46	188284	$-114.5 \pm 1.2$	$-119.8 \pm 1.2$	0.65	2.15	13.58

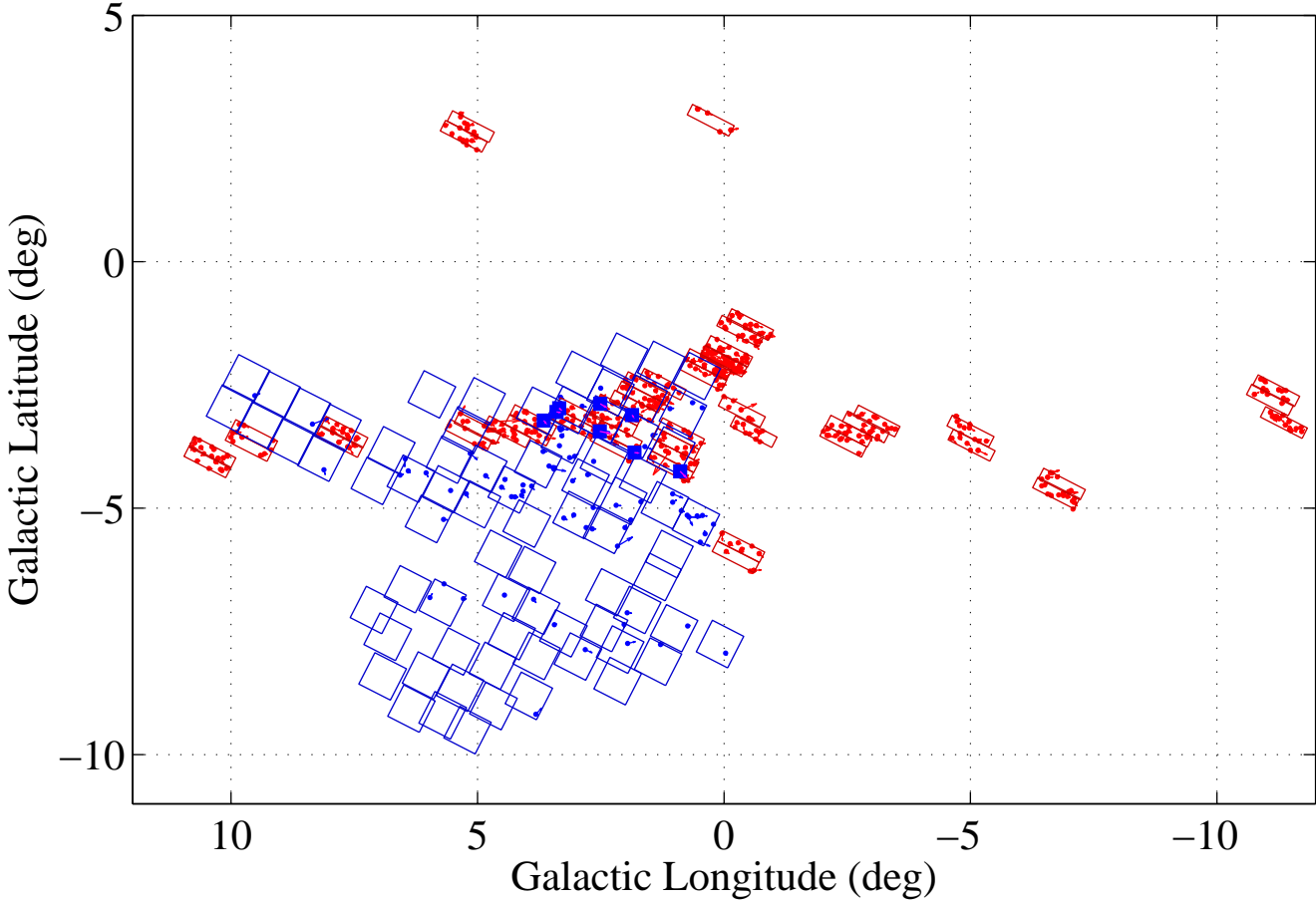


**Figure 2.** The MACHO (blue) and OGLE-II (red) Galactic bulge fields. The position and proper motion of known MACHO and candidate OGLE-II high proper motion stars are shown as blue and red points and arrows respectively. The 9 MACHO high proper motion stars which fall within the OGLE-II fields are shown as solid blue squares.

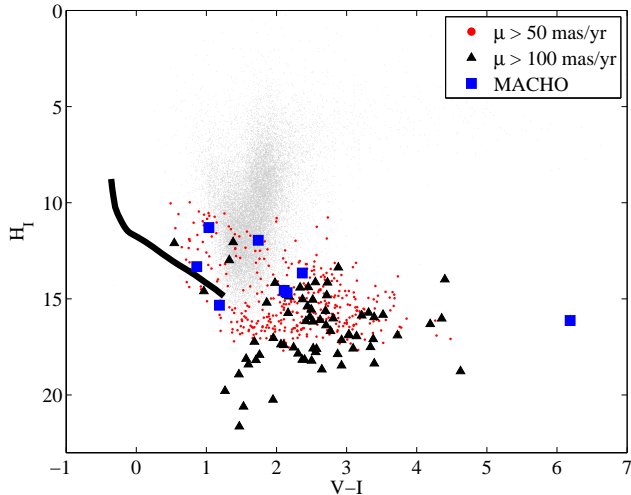


**Figure 3.** OGLE-II reduced proper motion as function of colour. The reduced proper motion for a subset of stars in OGLE bulge field SC 1 are shown in grey. Stars with proper motion  $\mu > 50 \text{ mas yr}^{-1}$  or  $\mu > 100 \text{ mas yr}^{-1}$  are shown as red dots and black triangles respectively. The 9 MACHO high proper motion stars which appear in the OGLE-II fields (and which are cross-identified with OGLE-II stars in Table 1) are shown as solid blue squares. The solid black line is derived from the theoretical luminosity model of a pure hydrogen white dwarf from Bergeron et al. (1995), located at a distance of 10 pc with a proper motion of  $100 \text{ mas yr}^{-1}$ .

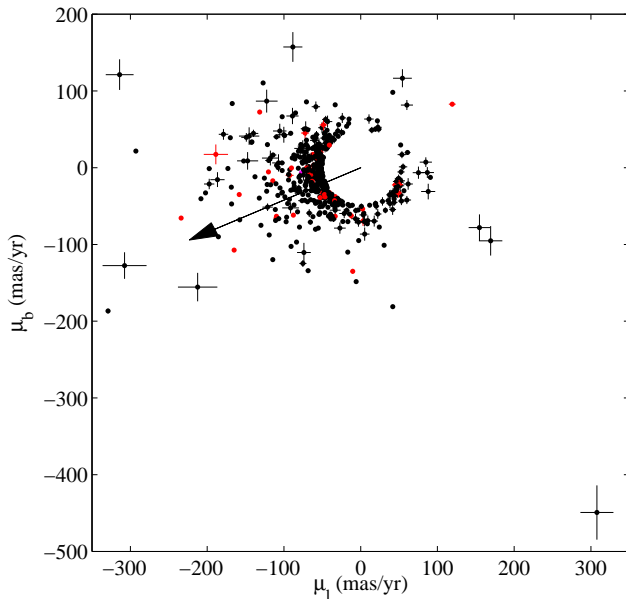


**Figure 4.** Proper motions in the Galactic co-ordinate longitude and latitude directions,  $\mu_l$ ,  $\mu_b$ , respectively for the 521 stars in the OGLE-II proper motion catalogue which have total proper motion  $\mu > 50 \text{ mas yr}^{-1}$  and  $\sigma_\mu/\mu < 0.1$ . The direction to the solar antapex is indicated with an arrow. Points in red correspond to stars which have photometrically determined distances of  $d < 50 \text{ pc}$ , see Section 5.

OGLE-II high proper motion candidate stars with the DENIS near infra-red survey.

The DENIS survey data base contains photometry in the optical band  $I$  ( $0.8 \mu\text{m}$ ), and the near-infrared bands  $J$  ( $1.25 \mu\text{m}$ ) and  $K_s$  ( $2.17 \mu\text{m}$ ) for the entire southern sky (Epchtein et al. 1997). The DENIS data base was searched for counterparts to stars in the sample of OGLE-II high proper motion stars. The DENIS data available online<sup>1</sup> use epoch J2000.0, corresponding to that used by the OGLE-II and MACHO catalogues. The OGLE-II data base has an internal positional accuracy of  $0.15 - 0.20 \text{ arcsec}$  and is cross-identified with the *Digital Sky Survey* (DSS) which has a maximum systematic error of  $0.7 \text{ arcsec}$  (Udalski et al. 2002). The most pessimistic  $3\sigma$  positional error for an OGLE-II star is therefore  $\simeq 3 \text{ arcsec}$ . The DENIS frames are referenced to the USNO-A2.0 catalogue which has a  $\sim 1 \text{ arcsec}$  accuracy (Phan-Bao et al. 2001). The DENIS  $3\sigma$  astrometric precision is also therefore  $\simeq 3 \text{ arcsec}$  (see also Reyl   and Robin 2004). The closest DENIS star within a search radius of  $(3^2 + 3^2)^{1/2} \simeq 4 \text{ arcsec}$  around each OGLE-II high proper motion star was determined. 241 OGLE-II high proper motion star candidates had counterparts in the DENIS database within an error circle of  $4 \text{ arcsec}$ .

## 5 PHOTOMETRIC DISTANCES

We plot the  $(I, I - J)$  colour-magnitude diagram for OGLE-II high proper motion candidate stars with likely DENIS counterparts in Figure 5. Based on the range of theoretical luminosity models (see below) we identify stars with colour  $I - J < 0.6$  as white dwarfs;  $0.6 < I - J < 1.0$  as G or K-dwarfs;  $1 < I - J < 3$  as M-dwarfs and stars with colour  $I - J > 3.0$  as possible brown dwarf candidates. Reyl   and Robin (2004) note that stars with  $I - J \lesssim 0.7$  can be either distant red dwarfs or close white dwarfs. The theoretical luminosity-colour relations for these different stellar types are also shown in Figure 5: for pure hydrogen white dwarfs (Bergeron et al. 1995); G/K dwarfs with metallicities  $[\text{Fe}/\text{H}] = 0.0, -1.0, -2.0$  and  $-2.5$  (Lejeune et al. 1997) and M dwarfs with metallicity  $[\text{Fe}/\text{H}] = 0.0$  (Baraffe et al. 1998). These theoretical models are used to derive distance estimates for the sample of high proper motion stars.

Tables 2 and 3 show the distance estimations for the stars which are classified as either G/K dwarfs (Table 2) or M dwarfs (Table 3), using the corresponding theoretical luminosity models. We note that in Table 2 there are up to four distance estimations for stars, depending on metallicity. Reyl   et al. (2002) use the Besan  on population synthesis model (Robin et al. 2003) to simulate the stellar populations in the direction of their high proper motion sample in order to discriminate between different Galactic populations. By identifying regions in the reduced proper motion-colour diagram corresponding to spheroid, thick disc and disc populations, Reyl   et al. (2002) were able to apply the most appropriate metallicity value for each star. A similar clear discrimination between Galactic stellar populations using the Besan  on model in the direction of the OGLE-II

<sup>1</sup> Vizier catalogue access tool, Centre de Donn  es astronomiques de Strasbourg

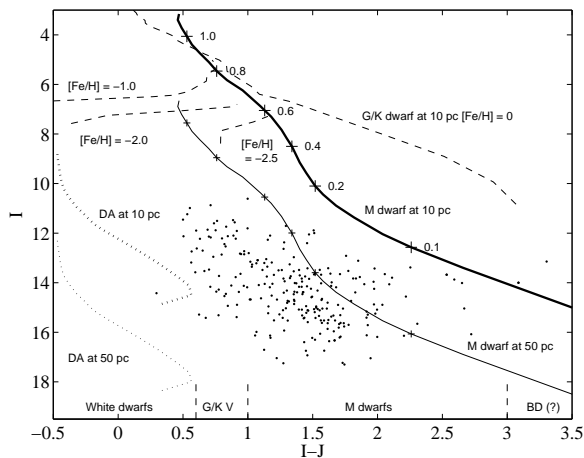


**Figure 5.** Colour magnitude diagram of OGLE-II high proper motion stars which have DENIS counterparts. The stellar type categorization of Reyl   et al. (2002) is indicated along the lower horizontal axis, where we identify stars with colour  $I - J < 0.6$  as white dwarfs;  $0.6 < I - J < 1.0$  as G or K-dwarfs;  $1 < I - J < 3$  as M-dwarfs and stars with colour  $I - J > 3.0$  as possible brown dwarf candidates. The heavy (light) solid black line shows the luminosity-colour relation of an M-dwarf at 10 (50) pc with solar metallicity using the theoretical model of Baraffe et al. (1998). The plus signs indicate stellar mass in solar units. The theoretical luminosity-colour relations for a hydrogen white dwarf (Bergeron et al. 1995) at 10 pc and 50 pc is shown as a dotted line. The series of dashed lines show the luminosity-colour relations for a G/K star at 10 pc with metallicities  $[\text{Fe}/\text{H}] = 0.0, -1.0, -2.0$  and  $-2.5$  Lejeune et al. (1997).

fields was not possible. Distances for G/K stars derived from all applicable theoretical models are therefore presented in Table 2, however we note that the metallicity for disk stars is most likely to be  $-1 \lesssim [\text{Fe}/\text{H}] \lesssim 0$  (Edvardsson et al. 1993; Ibukiyama and Arimoto 2002). For this reason, more weight should be given to the first two distance estimates in column 7 of Table 2. None of the stars in Table 2 is likely to have  $d < 50$  pc and are therefore not dealt with further in this study.

One star in the OGLE-II high proper motion sample has a DENIS  $I - J$  colour (0.3) and  $I$  band magnitude (14.42) consistent with a close white dwarf. The photometric distance determined using the bright main branch ( $I < 14$  for a white dwarf at 10 pc in Figure 5) of the theoretical luminosity model for a pure hydrogen white dwarf of Bergeron et al. (1995) is  $18^{+1}_{-1}$  pc. Using the faint branch gives a distance of  $4^{+1}_{-1}$  pc.

## 6 SEARCH FOR NEARBY COOL STARS

The 44 OGLE-II high proper motion star candidates with distances  $d < 50$  pc in Table 3 were cross-identified with entries in the 2MASS (Cutri et al. 2003) database of  $JHK_s$  photometry and are listed in Table 4<sup>2</sup>. 37 of these have

counterparts in the 2MASS database within an error circle of 1 arcsec. The photometry of bright stars in the DENIS catalogue potentially suffers effects due to saturation. We cross-identified our sample of DENIS objects with the 2MASS catalogue to obtain more accurate photometry, and to highlight instances of mis-identification. Furthermore, the 2MASS absolute astrometry accuracy is 70 - 80 mas for stars with  $9 < K_s < 14$  (Cutri et al. 2005).

A total of 270 OGLE-II high proper motion star candidates had counterparts in the 2MASS database within an error circle of 3 arcsec. We note however that the DENIS  $I$  magnitudes and  $I - J$  colour were required to apply the theoretical luminosity functions above.

## 7 DISCUSSION

Table 4 lists 43 stars with proper motion  $\mu > 50$  mas yr<sup>-1</sup>, distance  $< 50$  pc and stellar type consistent with late M dwarfs or early L type stars. The distance estimate is derived from the DENIS photometry, and the corresponding 2MASS colour and magnitude for these stars are consistent with cool dwarf stars. It is possible that a fast-moving nearby star in the OGLE-II proper motion catalogue has been falsely cross-identified with a distant red giant star in the DENIS catalogue. Categorizing this star as an M-dwarf on the basis of DENIS  $I - J$  colour would consequently result in a small distance, and thereby  $M_J$  values appearing to be consistent with those of late type M, or L stars. The majority of DENIS stars in Table 4 have a counterpart in the 2MASS catalogue within 1 arcsec. However, mis-identification is most likely to arise during the cross-identification between the OGLE-II and DENIS catalogues. We cross-identified OGLE-II stars with the DENIS catalogue entries using the most permissive ( $3\sigma$ ) position errors in each catalogue (Section 4). Given the crowded nature of the fields towards the Galactic Centre, it is likely that several OGLE-II high proper motion stars have been mis-identified in the DENIS catalogue, and consequently in the 2MASS catalogue. There are 8 stars in Table 4 which have both the positional difference between the OGLE-II and DENIS, and between the DENIS and 2MASS positions less than 1 arcsec. Ignoring possible co-ordinate reference frame offsets between the catalogues, these 8 high proper motion stars are least likely to have been misidentified in the IR catalogues based on position alone. These stars, with Unique ID (UID) numbers 7, 9, 16, 19, 29, 40, 43, 44 (See Table 4) have been indicated with a star symbol in the first column of both Tables 3 and 4.

Correctly cross-identified stars should have consistent magnitudes as well as position. We computed the difference between the  $J$  and  $K_s$  DENIS and 2MASS magnitudes for this set of 8 stars. The error in the magnitude difference is taken to be the sum in quadrature of the photometric errors. The DENIS and 2MASS  $J$  magnitudes are consistent at the  $1\sigma$  level for all stars except stars 7 and 9, which differ by  $2.5\sigma$  and  $3.4\sigma$  respectively. Stars 16, 29, 43 and 44 have DENIS and 2MASS  $K_s$  magnitudes consistent within  $1\sigma$ ; stars 9, 19 and 40 differ in  $K_s$  by  $1.7\sigma$ ,  $1.3\sigma$  and  $1.1\sigma$  respectively and no DENIS  $K_s$  magnitude is available for star 7. Carpenter (2001) gives relations for transforming DENIS  $K_s$  magnitudes and  $J - K_s$  colour to the 2MASS photometry system. The transformation produces a shift of  $< -0.02$

<sup>2</sup> Two of these stars, numbers 23 and 24 in Table 4 have almost identical OGLE-II positions and are treated as repeated entries.

mag on the DENIS  $J$  and  $K_s$  magnitudes. Including this photometry transformation results in the  $< 1\sigma$  consistency between DENIS and 2MASS magnitudes as above except for star 44 which has  $J$  band magnitudes different by  $1.1\sigma$ , and stars 9, 19, 29 and 40 which differ in  $K_s$  by  $2.0\sigma$ ,  $1.2\sigma$ ,  $1.1\sigma$  and  $1.3\sigma$  respectively. Phan-Bao et al. (2001) however notes that the Carpenter (2001) photometry transformations were derived using a small fraction of the total DENIS data. The increased disagreement between 2MASS and DENIS magnitudes arising from the application of these transformations may therefore be not significant. We note that blending within the seeing disks of both the 2MASS and DENIS experiments may account for small differences in photometry.

We therefore claim that stars 16, 19, 29, 40, 43 and 44 have been correctly cross-identified between the OGLE-II, DENIS and 2MASS catalogues, based on their consistent position and magnitudes which agree to within  $1.3\sigma$ . The entries for these 6 stars are indicated by a dagger symbol in Tables 3 and 4.

The absolute  $J$  band magnitude,  $M_J$ , and  $I - J$  colour for these 6 stars is shown in Figure 6, along with the photometry of late M-type and brown dwarf stars from Dahn et al. (2002). The absolute magnitude for the high proper motion stars is computed using the photometric distance estimates,  $d$ , and 2MASS  $J$  band magnitudes in Table 4. Large errors on the  $M_J$  values exist, largely arising from the uncertainty in photometric distance. Phan-Bao et al. (2001) noted that there is a significant scatter in the late type M-dwarf colour-luminosity relation of approximately  $\pm 1$  mag which corresponds to an average random error on every star of  $\sim 45\%$ . Phan-Bao et al. (2001) also find that a polynomial fit to the absolute  $I$ -band magnitudes as a function of  $I - J$  colour of their sample is up to  $\sim 1$  mag lower than the theoretical luminosity model of Baraffe et al. (1998). This difference is greatest for colours  $1.4 \lesssim I - J \lesssim 2.0$ , which encompasses the majority of M-dwarf stars in our sample. If the theoretical luminosity,  $M_I$  is overestimated by 1 mag for these stars, this corresponds to a systematic  $\sim 60\%$  underestimate of  $d$ . The lower errors on distance in Table 4 were computed from the sum in quadrature of the error due to DENIS  $I$ -band photometric uncertainties and the statistical scatter in the luminosity function. The upper distance error also includes in quadrature the systematic 60% uncertainty due to the possible underestimate in  $d$  arising from the theoretical luminosity model of Baraffe et al. (1998).

The colour and magnitude of the OGLE-II high proper motion stars in Figure 6 suggests the continuation of a well-defined trend seen in the cool dwarf data from Dahn et al. (2002). The two bluest (and earliest) dwarf stars in Dahn et al. (2002) have a spectral type of M6.5. All the OGLE-II nearby candidate stars are blue-ward of this, suggesting spectral types earlier than M6.5.

The  $I - J, V - I$  colour-colour diagram for this subsample of 6 stars is shown in Figure 7. The colours of these stars are consistent with the model colours from Baraffe et al. (1998), and continues the trend observed in the Dahn et al. (2002) data. We estimate the masses of these stars to be  $0.1M_\odot - 0.3M_\odot$ .

The star which has DENIS colour and magnitude consistent with a nearby white dwarf does not have a counterpart in the 2MASS catalogue within 5.9 arcsec.

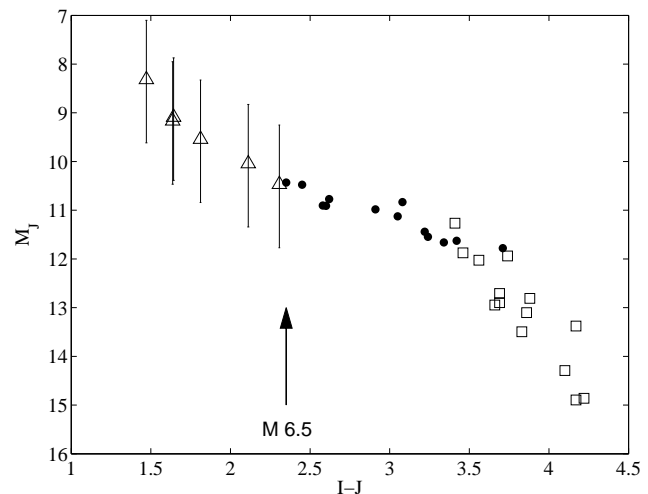


**Figure 6.** Comparison between candidate nearby high proper motion stars in the OGLE-II proper motion catalogue with cool dwarf and brown dwarf photometry from Dahn et al. (2002). Triangles indicate the  $J$ -band absolute magnitudes,  $M_J$  and  $I - J$  colours for OGLE-II high proper motion stars ( $\mu > 50 \text{ mas yr}^{-1}$ ) which have photometric distances  $d < 50$  pc and corresponding entries within 1 arcsec in the DENIS catalogue: stars 16, 19, 29, 40, 43 and 44 (UIDs, see Table 4 and text). The photometric data for late M-type stars from Dahn et al. (2002) are shown as circles and that for stars with later spectral type are shown as squares.

None of the members in the sample of candidate nearby ( $d < 50$  pc) high proper motion OGLE-II stars has corresponding entries in the *Catalogue of Nearby Stars* (CNS3, Gliese and Jahreiß 1991) or the catalogue of Woolley (1970). Both catalogues have a distance limit of 25 pc. Two stars in the set of 6 best-quality candidate nearby stars have distances within 25 pc (stars 9 and 16, see Table 4), however their absence from the CNS3 catalogue suggests that this is the first distance estimate for these stars. None of these stars have corresponding entries in the *Hipparcos/Tycho* catalogue (Perryman and ESA 1997). However, we note that the *Hipparcos* limiting magnitude is  $V = 12.4$  and the catalogue is complete down to  $V = 7.3 - 9.0$  mag (depending on colour) (Perryman et al. 1997). The *Tycho* catalogue has a limiting magnitude of  $V = 11.5$  and is (99.9%) complete to  $V = 10.0$  (Hoeg et al. 1997). The  $V$  band magnitudes of the candidate nearby stars ( $d < 50$  pc) in the OGLE-II high proper motion sample are  $V \gtrsim 15$ , too faint for *Hipparcos*.

We note that stars 13, 28 and 42 in Table 4 have photometric distances  $d < 10$  pc. This discovery of new nearby stars, if correct, is exciting. However, the closest DENIS counterparts to these OGLE-II HPM stars are at 3.01, 3.72 and 3.01 arcsecs respectively. Given the crowded nature of the Galactic bulge fields, mis-cross-identification remains a possibility that cannot be ruled out without higher resolution imaging of and around these stars.

## 8 CONCLUSION

The large scale microlensing survey conducted by the OGLE-II collaboration has produced proper motions for a large number of stars towards the Galactic Centre. A sample

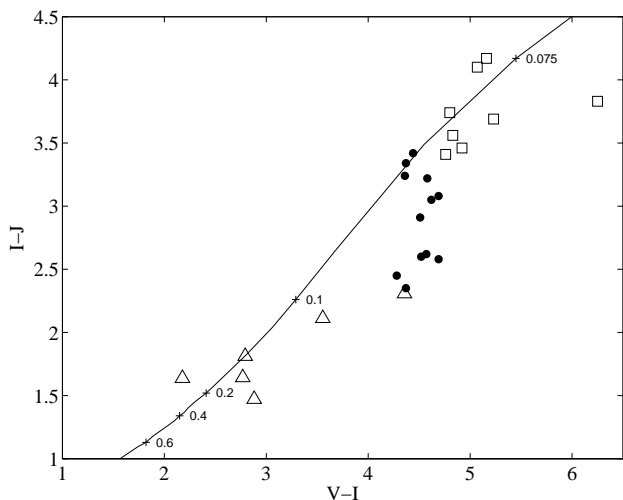


**Figure 7.**  $I - J$ ,  $V - I$  colour-colour relation for the sample of 6 best-quality OGLE-II high proper motion stars (triangles) with cool dwarf and brown dwarf photometry from Dahn et al. (2002) (see caption Figure 6 for explanation of symbols). The solid black line indicates the corresponding model with solar metallicity from Baraffe et al. (1998), with stellar masses indicated in solar units.

of stars with high proper motions  $\mu > 50 \text{ mas yr}^{-1}$  was extracted and cross-identified with the DENIS infrared survey database. Stars were identified as either G/K or M dwarf stars based on their DENIS  $I$ -band magnitude and  $I - J$  colour. Photometric distance estimates were derived using theoretical luminosity functions for the appropriate stellar type.

Nearby M-dwarf stars with photometric distances  $d < 50 \text{ pc}$  were selected and cross-indexed with the 2MASS catalogue. A set of 6 high proper motion stars had corresponding positions in the DENIS catalogue within 1 arcsec, cross-identified themselves with entries in the 2MASS catalogue within 1 arcsec. The DENIS and 2MASS  $J$  and  $K_s$  magnitudes of these stars are consistent to within  $1.3\sigma$ . The absolute  $J$  band magnitude  $M_J$  and  $I - J$  colour of these 6 stars continues a well-defined trend seen in the sample of late type nearby M and L dwarfs given in Dahn et al. (2002). Large uncertainties exist on the photometric distance estimation, arising from the observed intrinsic scatter in the luminosity and colour of M-dwarfs and the possible systematic overestimation of these stars' theoretical absolute magnitude. However, the comparison between the  $I - J$  colour of these 6 stars and the data from Dahn et al. (2002) suggest that these stars are M dwarfs with spectral type earlier than M6.5. The  $I - J$ ,  $V - I$  colour-colour relationship of these 6 stars clearly continues the trend seen in the Dahn et al. (2002) data, and is consistent with theoretical model predictions from Baraffe et al. (1998), suggesting masses for these stars approximately  $0.1M_{\odot} - 0.3M_{\odot}$ .

None of the candidate nearby ( $d < 50 \text{ pc}$ ) stars appear in the CNS3 or *Hipparcos/Tycho* catalogues. Most proper motion surveys do not cover the Galactic plane due to the high levels of extinction encountered. Extinction has not been accounted for in this work. While the effects of extinction is expected to be minimal for the nearest stars, ex-

tingtion is an additional source of uncertainty in the distance estimates for these stars.

The set of 6 nearby dwarf candidates was established by applying stringent cuts on proper motion accuracy and requiring good position and magnitude cross-identification. However, due to the crowded fields in which these stars were found, there remains a risk that these high proper motion stars have been mis-identified with stars in the DENIS and 2MASS catalogues.

It was not possible to derive reliable trigonometric distances to these stars as their location means their astrometric parallax signature is degenerate with that of differential refraction. In order to more accurately determine the stellar type of and thereby distance to these stars, low resolution spectroscopy is required. These stars would be an ideal target for optical or IR spectroscopy.

## ACKNOWLEDGMENTS

We thank C. Reyl , W. Evans, V. Belokurov and T. Sumi for helpful discussions. NJR acknowledges financial support by a PPARC PDRA fellowship. This work was partially supported by the European Community's Sixth Framework Marie Curie Research Training Network Programme, Contract No. MRTN-CT-2004-505183 'ANGLES'.

This publication makes use of data products from the Two Micron All Sky Survey, which is a joint project of the University of Massachusetts and the Infrared Processing and Analysis Center/California Institute of Technology, funded by the National Aeronautics and Space Administration and the National Science Foundation.

This research has made use of the Vizier catalogue access tool, CDS, Strasbourg, France.

Table 2: Photometric distance estimation of OGLE-II high proper motion stars with DENIS counterparts. Stars are characterized as G/K-dwarfs based on DENIS  $I - J$  colour, and distance estimate,  $d$ , determined using the theoretical luminosity model of Lejeune et al. (1997). Up to four distance estimations are given, corresponding to metallicities  $[\text{Fe}/\text{H}] = 0.0, -1.0, -2.0$  and  $-2.5$ ; however more weight should be given to the first two distance estimates, see text. Columns 1-2 are the OGLE-II field number and star ID.  $\mu_l$ ,  $\mu_b$  are the proper motions in Galactic longitude and latitude directions from the OGLE-II high proper motion catalogue.

Field	ID	$\mu_l \pm \sigma_{\mu_l}$ (mas yr <sup>-1</sup> )	$\mu_b \pm \sigma_{\mu_b}$ (mas yr <sup>-1</sup> )	$I$	$I - J$	$d$ (pc)	DENIS-ID
3	24531	43.29 $\pm$ 4.74	-37.43 $\pm$ 5.31	14.18	0.995	438/ - / - / 209	J175310.2-301747
3	147285	-72.90 $\pm$ 0.41	11.60 $\pm$ 0.39	14.36	0.757	756/ - / 303/ -	J175315.0-294440
3	287539	-49.31 $\pm$ 2.97	-29.76 $\pm$ 2.68	10.88	0.713	159/136/ 60/ -	J175328.1-300353
3	383035	-53.24 $\pm$ 0.45	-50.81 $\pm$ 0.48	12.17	0.714	288/250/110/ -	J175321.7-294013
4	13254	-75.46 $\pm$ 6.54	28.19 $\pm$ 7.54	11.90	0.602	288/144/ 95/ -	J175416.5-300455
5	222816	-82.73 $\pm$ 2.00	15.62 $\pm$ 1.66	11.24	0.533	230/ 97/ 69/ -	J175021.5-301249
6	319492	-52.71 $\pm$ 0.59	17.75 $\pm$ 0.68	12.14	0.700	287/223/108/ -	J180814.4-320952
6	443524	-54.00 $\pm$ 0.37	-15.87 $\pm$ 0.41	14.94	0.846	775/ - / 401/ 268	J180826.1-321010
8	18351	-56.42 $\pm$ 0.48	-30.47 $\pm$ 0.47	14.11	0.873	509/ - / 279/ 187	J182243.1-220530
8	57591	-68.29 $\pm$ 0.57	-35.56 $\pm$ 0.56	14.37	0.931	526/ - / - / 219	J182242.1-214402
8	285968	-29.89 $\pm$ 0.57	-48.44 $\pm$ 0.62	12.74	0.567	442/202/138/ -	J182312.1-213256
9	27834	-41.03 $\pm$ 0.75	-38.52 $\pm$ 1.02	11.74	0.833	200/ - / 92/ 61	J182342.4-215658
9	54021	53.13 $\pm$ 4.61	-43.33 $\pm$ 5.37	15.42	0.676	1333/807/485/ -	J182333.4-213921
9	279206	-68.79 $\pm$ 0.82	-8.47 $\pm$ 0.72	14.16	0.711	723/612/274/ -	J182429.3-215312
10	352468	-49.91 $\pm$ 1.95	4.85 $\pm$ 1.62	12.10	0.889	197/ - / 112/ 75	J182031.3-224929
13	25882	-48.01 $\pm$ 2.24	-25.81 $\pm$ 1.88	14.28	0.776	715/ - / 293/ -	J181640.8-241520
13	315786	-75.25 $\pm$ 4.67	-124.77 $\pm$ 4.55	10.61	0.999	84/ - / - / 40	J181706.2-241152
13	563636	-45.57 $\pm$ 4.70	62.92 $\pm$ 4.59	13.19	0.564	545/247/170/ -	J181718.9-233259
14	136405	-59.59 $\pm$ 1.01	27.17 $\pm$ 0.99	13.77	0.906	414/ - / 245/ 163	J174633.0-224901
16	65346	-121.42 $\pm$ 0.70	30.17 $\pm$ 0.73	15.29	0.624	1334/708/452/ -	J180937.7-262350
16	501033	6.83 $\pm$ 0.86	-69.54 $\pm$ 0.77	12.23	0.907	203/ - / 120/ 80	J181011.8-255821
16	543398	-125.42 $\pm$ 0.92	-13.62 $\pm$ 0.89	12.13	0.504	358/144/103/ -	J181032.7-264204
18	51131	-37.10 $\pm$ 0.53	-47.98 $\pm$ 0.55	12.83	0.940	255/ - / - / 108	J180635.3-272354
18	642493	-35.86 $\pm$ 0.64	-45.68 $\pm$ 0.68	12.54	0.829	291/ - / 133/ 88	J180734.4-271940
19	73428	-34.29 $\pm$ 0.68	-48.84 $\pm$ 0.62	12.54	0.829	291/ - / 133/ 88	J180734.4-271940
20	775068	-55.15 $\pm$ 0.49	-29.18 $\pm$ 0.48	13.73	0.778	553/ - / 227/ -	J175937.7-282547
22	413569	-63.30 $\pm$ 0.43	-25.52 $\pm$ 0.46	12.21	0.801	264/ - / 114/ 74	J175700.7-310318
24	77382	-45.86 $\pm$ 0.63	-20.86 $\pm$ 0.71	11.86	0.690	256/183/ 95/ -	J175254.8-325010
25	438478	-53.46 $\pm$ 0.96	-19.08 $\pm$ 1.26	11.88	0.752	243/209/ 97/ -	J175438.3-323401
26	165925	-69.39 $\pm$ 0.55	-44.44 $\pm$ 0.51	14.54	0.820	744/ - / 333/ 220	J174645.8-343514
28	83963	-169.87 $\pm$ 1.91	39.15 $\pm$ 1.68	11.51	0.763	202/ - / 81/ -	J174641.4-364847
28	84079	-178.76 $\pm$ 6.18	43.54 $\pm$ 7.03	11.51	0.763	202/ - / 81/ -	J174641.4-364847
31	124959	-41.53 $\pm$ 2.78	-32.29 $\pm$ 3.88	13.47	0.701	530/414/199/ -	J180158.6-282843
31	765538	-110.95 $\pm$ 0.60	-68.70 $\pm$ 0.60	14.13	0.969	444/ - / - / 200	J180243.3-281355
33	771	-67.65 $\pm$ 0.94	-8.80 $\pm$ 1.03	15.39	0.914	861/ - / 519/ 345	J180507.4-291905
33	365983	-58.09 $\pm$ 0.48	-31.30 $\pm$ 0.49	13.53	0.665	564/333/203/ -	J180516.9-282951
36	648617	-32.92 $\pm$ 0.49	43.85 $\pm$ 0.52	13.64	0.944	369/ - / - / 158	J180534.2-273148
37	181412	-53.67 $\pm$ 1.02	12.11 $\pm$ 0.98	11.60	0.739	216/177/ 85/ -	J175228.1-301557
38	45507	-37.57 $\pm$ 0.74	-34.68 $\pm$ 0.77	11.91	0.915	173/ - / 105/ 70	J180110.2-300803
39	222196	-74.38 $\pm$ 0.52	-2.69 $\pm$ 0.53	12.12	0.846	212/ - / 110/ 73	J175533.7-301125
39	387848	-44.83 $\pm$ 3.44	-30.74 $\pm$ 2.75	10.98	0.553	200/ 88/ 62/ -	J175531.7-292516
40	246654	-67.89 $\pm$ 0.46	-6.69 $\pm$ 0.54	12.85	0.948	254/ - / - / 109	J175051.7-331230
40	452942	-68.36 $\pm$ 0.52	25.24 $\pm$ 0.55	12.71	0.652	393/224/139/ -	J175114.6-325536
41	16970	-56.46 $\pm$ 0.50	-9.61 $\pm$ 0.49	14.45	0.831	701/ - / 320/ 213	J175139.9-332813
41	473835	-95.23 $\pm$ 0.50	-46.73 $\pm$ 0.51	12.73	0.972	232/ - / - / 105	J175233.6-332631
41	503739	-68.47 $\pm$ 2.94	-134.26 $\pm$ 2.52	11.57	0.899	152/ - / 88/ 59	J175238.9-331449
42	445360	-57.07 $\pm$ 0.97	-44.35 $\pm$ 0.98	11.81	0.998	146/ - / - / 70	J180908.7-263004
44	265613	-29.96 $\pm$ 0.48	-46.23 $\pm$ 0.52	12.62	0.606	399/202/132/ -	J174945.1-300610
45	10225	-51.10 $\pm$ 0.86	-3.74 $\pm$ 0.97	12.44	0.820	284/ - / 127/ 84	J180314.7-302919
46	26214	-109.74 $\pm$ 4.29	40.18 $\pm$ 3.24	11.47	0.886	148/ - / 84/ 56	J180408.1-302031
46	298227	-139.69 $\pm$ 6.23	44.77 $\pm$ 4.70	12.96	0.734	405/349/158/ -	J180455.3-303057
47	23616	-59.23 $\pm$ 1.61	-7.29 $\pm$ 1.52	14.89	0.917	682/ - / 414/ 275	J172627.8-395651
47	28899	-50.05 $\pm$ 1.11	9.08 $\pm$ 1.47	13.58	0.595	630/310/205/ -	J172639.2-395338



Table 2 continued

Field	ID	$\mu_l \pm \sigma_{\mu_l}$ (mas yr <sup>-1</sup> )	$\mu_b \pm \sigma_{\mu_b}$ (mas yr <sup>-1</sup> )	$I$	$I - J$	$d$ (pc)	DENIS-ID
47	141928	-58.29 $\pm$ 1.26	38.87 $\pm$ 1.13	12.86	0.798	359/ - /153/100	J172657.6-392324
47	163215	-57.10 $\pm$ 0.71	0.17 $\pm$ 0.72	15.31	0.774	1153/ - /471/ -	J172714.5-400421
49	152288	-29.27 $\pm$ 0.82	40.82 $\pm$ 0.91	12.23	0.631	323/175/111/ -	J172939.0-402629
49	152290	-49.12 $\pm$ 0.82	-11.10 $\pm$ 0.87	12.85	0.972	246/ - / - /112	J172940.1-402623

Table 3: Photometric distance estimation of OGLE-II high proper motion stars with DENIS counterparts. Stars are characterized as M-dwarfs based on DENIS  $I - J$  colour. The distance  $d$  is determined using the theoretical luminosity model of Baraffe et al. (1998) for a solar metallicity star with errors derived from the uncertainty in the reported  $I$ -band magnitudes. Columns 1-2 are the OGLE-II field number and star ID.  $\mu_l$ ,  $\mu_b$  are the proper motions in Galactic longitude and latitude directions from the OGLE-II high proper motion catalogue. See Section 7 for an explanation of the star and dagger symbols in column 1.

Field	ID	$\mu_l \pm \sigma_{\mu_l}$ (mas yr <sup>-1</sup> )	$\mu_b \pm \sigma_{\mu_b}$ (mas yr <sup>-1</sup> )	$I$	$I - J$	$d$ (pc)	DENIS-ID
1	202039	-64.28 $\pm$ 0.58	-29.93 $\pm$ 0.66	15.01	1.527	94 <sup>+3</sup> <sub>-3</sub>	J180219.8-301955
1	238184	45.12 $\pm$ 4.47	-30.93 $\pm$ 6.12	15.16	1.916	50 <sup>+2</sup> <sub>-2</sub>	J180222.9-301005
1	587955	-44.03 $\pm$ 3.42	-26.51 $\pm$ 3.09	15.31	1.713	72 <sup>+3</sup> <sub>-3</sub>	J180250.1-301340
1	619578	8.66 $\pm$ 2.46	-73.00 $\pm$ 2.74	15.04	1.609	78 <sup>+3</sup> <sub>-3</sub>	J180249.0-300128
1	701357	-92.55 $\pm$ 5.20	-9.90 $\pm$ 4.33	13.48	1.555	43 <sup>+1</sup> <sub>-1</sub>	J180259.7-293831
2	413124	-72.61 $\pm$ 0.86	20.75 $\pm$ 0.75	15.11	1.461	123 <sup>+4</sup> <sub>-4</sub>	J180417.4-282734
2	426502	-56.39 $\pm$ 5.29	17.54 $\pm$ 5.03	12.91	1.758	22 <sup>+1</sup> <sub>-1</sub>	J180429.7-291729
3	64760	2.99 $\pm$ 6.52	-69.43 $\pm$ 6.51	15.09	1.997	43 <sup>+2</sup> <sub>-2</sub>	J175301.9-300832
3	216180	-61.62 $\pm$ 5.49	2.65 $\pm$ 4.50	13.38	2.253	15 <sup>+1</sup> <sub>-1</sub>	J175330.8-302535
3	229801	44.99 $\pm$ 4.38	-22.30 $\pm$ 4.80	13.65	2.056	21 <sup>+1</sup> <sub>-1</sub>	J175327.9-301913
3	301228	-51.62 $\pm$ 5.06	9.91 $\pm$ 4.20	13.26	1.323	96 <sup>+2</sup> <sub>-2</sub>	J175323.5-295901
3*	370016	-164.93 $\pm$ 0.90	-107.34 $\pm$ 1.00	13.83	1.834	30 <sup>+1</sup> <sub>-1</sub>	J175329.3-294140
4	230257	-49.96 $\pm$ 0.60	-6.48 $\pm$ 0.71	13.15	1.020	215 <sup>+6</sup> <sub>-5</sub>	J175426.5-300256
4	231890	-52.81 $\pm$ 4.75	20.29 $\pm$ 5.00	14.39	1.829	40 <sup>+2</sup> <sub>-2</sub>	J175431.3-300158
4*	254212	-131.63 $\pm$ 1.99	72.61 $\pm$ 2.73	11.89	1.508	24 <sup>+1</sup> <sub>-1</sub>	J175429.1-295718
4	421737	-105.40 $\pm$ 8.75	47.93 $\pm$ 9.43	14.90	1.696	61 <sup>+2</sup> <sub>-2</sub>	J175441.2-300520
4	464317	-52.12 $\pm$ 5.45	27.58 $\pm$ 5.86	12.81	1.007	188 <sup>+4</sup> <sub>-4</sub>	J175442.7-295344
4	614523	-72.49 $\pm$ 5.16	45.21 $\pm$ 6.71	13.43	1.977	21 <sup>+1</sup> <sub>-1</sub>	J175454.4-300223
4	623507	-82.21 $\pm$ 0.44	-57.50 $\pm$ 0.47	13.66	1.511	53 <sup>+2</sup> <sub>-2</sub>	J175453.8-295925
4	625701	-48.45 $\pm$ 5.16	55.79 $\pm$ 8.22	14.89	2.038	37 <sup>+2</sup> <sub>-2</sub>	J175457.0-300005
4	734288	-188.71 $\pm$ 15.85	17.44 $\pm$ 12.94	15.04	2.669	21 <sup>+1</sup> <sub>-1</sub>	J175503.6-292621
5	38999	-38.77 $\pm$ 1.57	-40.39 $\pm$ 1.86	14.00	3.087	9 <sup>+1</sup> <sub>-1</sub>	J174950.1-300004
5	208658	-57.71 $\pm$ 0.42	27.11 $\pm$ 0.51	14.01	2.652	13 <sup>+1</sup> <sub>-1</sub>	J175027.5-301923
5	244353	-10.38 $\pm$ 2.80	-134.98 $\pm$ 3.20	16.08	2.723	32 <sup>+2</sup> <sub>-2</sub>	J175036.2-300145
5	314114	-55.19 $\pm$ 0.38	-78.68 $\pm$ 0.40	13.81	1.325	123 <sup>+2</sup> <sub>-2</sub>	J175046.2-302213
5	372152	30.62 $\pm$ 0.52	-101.08 $\pm$ 0.57	13.83	1.416	81 <sup>+2</sup> <sub>-2</sub>	J175051.3-295803
6	30011	-57.46 $\pm$ 0.65	-25.04 $\pm$ 0.64	14.96	1.159	357 <sup>+11</sup> <sub>-10</sub>	J180732.1-321842
6	351465	-52.31 $\pm$ 0.52	-39.74 $\pm$ 0.49	14.18	1.170	244 <sup>+6</sup> <sub>-6</sub>	J180819.4-315412
7	356532	-48.59 $\pm$ 1.04	-38.63 $\pm$ 1.04	16.22	1.175	617 <sup>+27</sup> <sub>-26</sub>	J180942.6-323124
8	50479	-51.31 $\pm$ 0.90	-1.10 $\pm$ 0.83	16.74	1.589	178 <sup>+10</sup> <sub>-9</sub>	J182249.2-214745
8*,†	98776	-12.37 $\pm$ 3.27	-62.42 $\pm$ 4.06	13.80	2.112	21 <sup>+1</sup> <sub>-1</sub>	J182247.8-212100
8	197686	90.86 $\pm$ 0.60	-12.55 $\pm$ 0.70	13.95	1.418	85 <sup>+2</sup> <sub>-2</sub>	J182305.6-212328
8	240063	-119.22 $\pm$ 1.41	-87.68 $\pm$ 1.87	12.37	1.280	75 <sup>+1</sup> <sub>-1</sub>	J182320.7-215712
8	350020	-50.64 $\pm$ 1.73	-31.68 $\pm$ 2.11	13.68	1.565	46 <sup>+1</sup> <sub>-1</sub>	J182326.3-214906
8	397026	24.30 $\pm$ 0.80	-77.33 $\pm$ 0.78	16.18	1.715	107 <sup>+4</sup> <sub>-4</sub>	J182329.4-212300
9	5893	-65.82 $\pm$ 0.54	-12.08 $\pm$ 0.62	16.40	1.435	245 <sup>+10</sup> <sub>-9</sub>	J182346.4-221211
9	68237	-68.36 $\pm$ 0.58	-7.54 $\pm$ 0.56	15.52	1.563	108 <sup>+3</sup> <sub>-3</sub>	J182336.9-212713
9	177063	-15.63 $\pm$ 0.50	57.80 $\pm$ 0.53	16.06	1.558	140 <sup>+5</sup> <sub>-5</sub>	J182408.1-220828
9	304725	-53.50 $\pm$ 0.88	3.11 $\pm$ 1.03	15.32	1.419	158 <sup>+11</sup> <sub>-10</sub>	J182422.8-213618
10	7699	-54.28 $\pm$ 0.93	-7.97 $\pm$ 0.87	16.71	1.126	862 <sup>+37</sup> <sub>-36</sub>	J181942.3-224617
10	92354	-98.88 $\pm$ 1.88	-37.97 $\pm$ 1.82	17.30	1.745	172 <sup>+11</sup> <sub>-10</sub>	J181944.2-220635
10	106322	-67.70 $\pm$ 0.66	15.29 $\pm$ 0.62	14.74	1.359	162 <sup>+4</sup> <sub>-4</sub>	J181951.2-220045
10	441733	-92.28 $\pm$ 1.53	-2.61 $\pm$ 1.23	15.52	1.202	416 <sup>+244</sup> <sub>-154</sub>	J182032.9-220222
11	121881	-64.58 $\pm$ 2.03	-9.95 $\pm$ 2.79	15.04	1.734	62 <sup>+2</sup> <sub>-2</sub>	J182105.0-224434

Table 3 continued

Field	ID	$\mu_1 \pm \sigma_{\mu_1}$ (mas yr <sup>-1</sup> )	$\mu_b \pm \sigma_{\mu_b}$ (mas yr <sup>-1</sup> )	$I$	$I - J$	$d$ (pc)	DENIS-ID
11	314503	-50.26 $\pm$ 1.62	6.81 $\pm$ 1.53	15.63	1.616	101 <sup>+3</sup> <sub>-3</sub>	J182112.1-215905
11	341519	-58.53 $\pm$ 0.57	-28.50 $\pm$ 0.59	13.22	1.066	200 <sup>+3</sup> <sub>-3</sub>	J182122.3-224108
11	409511	-10.78 $\pm$ 2.79	-48.89 $\pm$ 3.04	15.81	1.701	93 <sup>+4</sup> <sub>-3</sub>	J182125.3-220342
12	51118	-33.20 $\pm$ 1.66	-37.58 $\pm$ 2.09	13.12	1.851	21 <sup>+1</sup> <sub>-1</sub>	J181541.4-240408
12	96416	-32.53 $\pm$ 2.07	-43.47 $\pm$ 3.07	14.15	1.456	81 <sup>+2</sup> <sub>-2</sub>	J181548.0-234523
12	206648	-78.01 $\pm$ 2.79	30.14 $\pm$ 3.08	15.62	1.571	111 <sup>+4</sup> <sub>-4</sub>	J181552.0-235439
12	300639	-67.88 $\pm$ 0.55	1.62 $\pm$ 0.53	13.48	1.113	202 <sup>+4</sup> <sub>-4</sub>	J181610.3-241424
12	317171	-14.68 $\pm$ 0.46	-60.23 $\pm$ 0.48	14.39	1.380	123 <sup>+3</sup> <sub>-3</sub>	J181621.4-240520
12	373469	-168.15 $\pm$ 0.65	-47.15 $\pm$ 0.69	16.19	1.998	71 <sup>+4</sup> <sub>-3</sub>	J181617.3-234339
12	492778	-67.20 $\pm$ 1.29	-13.68 $\pm$ 1.26	13.09	1.076	184 <sup>+4</sup> <sub>-4</sub>	J181636.0-234538
12	493160	-70.56 $\pm$ 1.96	-17.01 $\pm$ 1.39	16.33	1.669	125 <sup>+6</sup> <sub>-6</sub>	J181635.1-234542
13	98184	-68.53 $\pm$ 0.71	-13.94 $\pm$ 0.81	13.09	1.076	184 <sup>+4</sup> <sub>-4</sub>	J181636.0-234538
13	98450	-78.63 $\pm$ 1.51	-17.89 $\pm$ 1.06	16.33	1.669	125 <sup>+6</sup> <sub>-6</sub>	J181635.1-234542
13	413466	-48.39 $\pm$ 0.76	13.41 $\pm$ 0.70	14.95	1.450	119 <sup>+3</sup> <sub>-3</sub>	J181711.4-233504
14	417830	-52.23 $\pm$ 0.69	-0.94 $\pm$ 0.71	12.10	1.172	93 <sup>+2</sup> <sub>-2</sub>	J174703.0-225835
14*,†	525442	-87.78 $\pm$ 0.92	-61.73 $\pm$ 1.11	15.66	2.307	40 <sup>+2</sup> <sub>-2</sub>	J174719.4-231412
14	545918	-127.05 $\pm$ 1.24	110.43 $\pm$ 0.96	15.59	1.462	153 <sup>+6</sup> <sub>-5</sub>	J174721.8-230445
15	40035	-88.56 $\pm$ 2.04	-28.55 $\pm$ 1.73	15.71	1.925	63 <sup>+3</sup> <sub>-3</sub>	J174736.7-231945
15	309307	-54.96 $\pm$ 2.48	21.05 $\pm$ 1.86	15.42	1.522	115 <sup>+5</sup> <sub>-5</sub>	J174806.6-224018
15	371749	-87.07 $\pm$ 1.00	-19.86 $\pm$ 1.49	14.75	1.317	195 <sup>+9</sup> <sub>-8</sub>	J174817.3-231154
15	470245	-71.40 $\pm$ 0.97	-2.65 $\pm$ 1.08	14.05	1.130	251 <sup>+10</sup> <sub>-10</sub>	J174832.7-232803
15	521758	-70.25 $\pm$ 1.63	-0.06 $\pm$ 1.58	13.99	1.647	44 <sup>+2</sup> <sub>-2</sub>	J174832.0-230851
15	557293	-16.67 $\pm$ 0.49	-70.29 $\pm$ 0.46	14.16	1.415	94 <sup>+4</sup> <sub>-4</sub>	J174825.9-225216
16	41668	-44.35 $\pm$ 0.49	-27.79 $\pm$ 0.58	14.38	1.428	99 <sup>+2</sup> <sub>-2</sub>	J180948.4-263009
16	319688	-53.08 $\pm$ 0.50	-16.73 $\pm$ 0.49	14.38	1.425	100 <sup>+2</sup> <sub>-2</sub>	J180959.5-260305
17	115581	-81.21 $\pm$ 0.73	-0.63 $\pm$ 0.61	15.93	1.280	385 <sup>+85</sup> <sub>-70</sub>	J181040.8-260435
17	395098	46.73 $\pm$ 4.73	-17.95 $\pm$ 5.77	15.06	1.539	93 <sup>+3</sup> <sub>-3</sub>	J181112.9-262949
17	566438	-75.45 $\pm$ 0.51	-34.81 $\pm$ 0.52	13.18	1.185	148 <sup>+3</sup> <sub>-3</sub>	J181128.5-262343
18	555084	-30.16 $\pm$ 0.97	-39.90 $\pm$ 0.79	14.63	1.102	351 <sup>+10</sup> <sub>-10</sub>	J180712.2-265031
19	202597	-172.97 $\pm$ 1.02	-1.00 $\pm$ 1.21	15.52	1.588	102 <sup>+3</sup> <sub>-3</sub>	J180752.3-273740
19	236380	-56.14 $\pm$ 2.02	-2.62 $\pm$ 1.92	15.53	1.673	86 <sup>+3</sup> <sub>-3</sub>	J180800.3-272746
19	258847	-55.23 $\pm$ 0.44	-14.93 $\pm$ 0.45	14.56	2.219	26 <sup>+1</sup> <sub>-1</sub>	J180753.1-272126
19	450718	-54.86 $\pm$ 4.78	16.80 $\pm$ 7.18	13.74	1.442	70 <sup>+2</sup> <sub>-2</sub>	J180803.8-271759
19	470116	-57.04 $\pm$ 0.47	26.99 $\pm$ 0.44	14.68	1.022	432 <sup>+11</sup> <sub>-10</sub>	J180805.9-271202
20	445532	49.24 $\pm$ 4.67	-32.80 $\pm$ 5.98	13.53	1.775	29 <sup>+1</sup> <sub>-1</sub>	J175934.3-291030
20	596512	-109.77 $\pm$ 1.22	-63.35 $\pm$ 1.45	13.68	2.533	13 <sup>+1</sup> <sub>-1</sub>	J175949.8-291926
20	625107	-307.64 $\pm$ 28.69	-127.48 $\pm$ 17.38	14.65	1.572	71 <sup>+2</sup> <sub>-2</sub>	J175935.6-291157
20	632206	-71.79 $\pm$ 1.51	-23.48 $\pm$ 1.63	13.05	1.142	154 <sup>+3</sup> <sub>-3</sub>	J175948.0-290733
20	764809	-54.03 $\pm$ 3.93	7.63 $\pm$ 4.69	15.32	1.660	80 <sup>+3</sup> <sub>-3</sub>	J175949.1-283047
21	140	-110.20 $\pm$ 1.40	-65.89 $\pm$ 1.71	13.68	2.533	13 <sup>+1</sup> <sub>-1</sub>	J175949.8-291926
21	254557	-45.24 $\pm$ 3.00	31.95 $\pm$ 3.00	15.37	1.644	84 <sup>+3</sup> <sub>-3</sub>	J180021.9-291515
21	298351	-212.48 $\pm$ 25.65	-155.58 $\pm$ 18.58	15.11	1.271	274 <sup>+9</sup> <sub>-9</sub>	J180012.0-290346
21	323807	-46.00 $\pm$ 0.43	-36.19 $\pm$ 0.46	14.40	1.277	193 <sup>+5</sup> <sub>-5</sub>	J180017.0-285728
21	379680	-43.24 $\pm$ 0.54	41.45 $\pm$ 0.56	13.27	1.033	221 <sup>+5</sup> <sub>-5</sub>	J180022.0-284122
21	422978	-60.61 $\pm$ 1.92	26.60 $\pm$ 2.18	14.52	1.184	275 <sup>+7</sup> <sub>-7</sub>	J180016.3-283333
21	480442	23.64 $\pm$ 3.66	50.41 $\pm$ 4.50	17.05	1.947	114 <sup>+8</sup> <sub>-7</sub>	J180022.2-291607
21	649329	-114.46 $\pm$ 0.48	-17.12 $\pm$ 0.50	13.41	1.620	36 <sup>+1</sup> <sub>-1</sub>	J180023.9-282744
22	155458	-70.72 $\pm$ 0.98	35.92 $\pm$ 1.45	16.14	2.204	55 <sup>+2</sup> <sub>-2</sub>	J175620.1-303231
22	681768	-40.85 $\pm$ 1.15	29.50 $\pm$ 1.44	15.25	1.983	47 <sup>+2</sup> <sub>-2</sub>	J175705.2-303146
23	63756	-73.23 $\pm$ 1.77	-4.45 $\pm$ 1.68	13.63	1.518	51 <sup>+1</sup> <sub>-1</sub>	J175726.3-312132
23	281219	-33.18 $\pm$ 2.59	-63.29 $\pm$ 2.77	14.74	1.797	49 <sup>+2</sup> <sub>-2</sub>	J175740.8-311443
23	339709	-16.76 $\pm$ 0.53	-109.97 $\pm$ 0.50	15.96	1.663	107 <sup>+5</sup> <sub>-5</sub>	J175748.2-305717
23	534675	-58.43 $\pm$ 2.63	-23.89 $\pm$ 1.86	16.12	1.917	77 <sup>+4</sup> <sub>-4</sub>	J175757.6-304930
24	201442	-147.36 $\pm$ 13.76	8.91 $\pm$ 11.46	16.21	1.708	110 <sup>+5</sup> <sub>-5</sub>	J175311.8-330610
24	266528	-114.14 $\pm$ 4.41	16.47 $\pm$ 3.05	15.62	1.715	83 <sup>+3</sup> <sub>-3</sub>	J175314.9-324129
24	334946	-55.86 $\pm$ 0.40	-31.26 $\pm$ 0.47	12.63	1.276	86 <sup>+2</sup> <sub>-2</sub>	J175331.8-331227
25	327263	-56.25 $\pm$ 0.39	12.27 $\pm$ 0.43	13.14	3.304	5 <sup>+1</sup> <sub>-1</sub>	J175441.4-331626
25*,†	592433	-158.28 $\pm$ 0.77	-35.01 $\pm$ 0.98	12.05	1.472	29 <sup>+1</sup> <sub>-1</sub>	J175443.1-323213

Table 3 continued

Field	ID	$\mu_l \pm \sigma_{\mu_l}$ (mas yr <sup>-1</sup> )	$\mu_b \pm \sigma_{\mu_b}$ (mas yr <sup>-1</sup> )	$I$	$I - J$	$d$ (pc)	DENIS-ID
26	165846	-54.27 $\pm$ 0.85	7.91 $\pm$ 0.93	14.10	1.085	286 <sup>+4</sup> <sub>-4</sub>	J174641.8-343514
26	275718	-106.83 $\pm$ 3.15	-66.45 $\pm$ 2.71	13.54	1.354	95 <sup>+2</sup> <sub>-2</sub>	J174700.9-345618
26	340032	-75.97 $\pm$ 1.00	21.38 $\pm$ 1.30	15.28	1.244	327 <sup>+8</sup> <sub>-8</sub>	J174706.4-343934
26	585326	-47.81 $\pm$ 4.78	38.55 $\pm$ 6.74	15.98	1.067	713 <sup>+24</sup> <sub>-23</sub>	J174739.7-351428
26	604525	-65.52 $\pm$ 6.45	-3.94 $\pm$ 5.40	15.23	1.157	407 <sup>+10</sup> <sub>-10</sub>	J174743.7-350905
27	152097	-61.08 $\pm$ 0.54	3.88 $\pm$ 0.57	15.09	1.417	143 <sup>+3</sup> <sub>-3</sub>	J174756.9-345017
28	77323	-52.28 $\pm$ 0.53	-19.20 $\pm$ 0.53	16.23	1.497	181 <sup>+6</sup> <sub>-6</sub>	J174636.7-365044
28	229742	-58.83 $\pm$ 0.45	-46.38 $\pm$ 0.48	13.49	1.262	134 <sup>+2</sup> <sub>-2</sub>	J174711.4-372123
28	285427	-109.54 $\pm$ 0.46	3.11 $\pm$ 0.52	15.03	1.294	241 <sup>+5</sup> <sub>-5</sub>	J174714.8-364840
28	328487	-62.11 $\pm$ 1.66	-2.51 $\pm$ 1.52	16.13	1.172	596 <sup>+23</sup> <sub>-22</sub>	J174724.7-371933
29	7843	-2.59 $\pm$ 0.38	-94.98 $\pm$ 0.46	15.67	1.704	87 <sup>+3</sup> <sub>-3</sub>	J174743.7-372955
29	39198	-44.61 $\pm$ 0.73	-22.85 $\pm$ 0.61	15.53	1.308	287 <sup>+9</sup> <sub>-8</sub>	J174751.6-371522
29	39202	-292.94 $\pm$ 0.73	21.67 $\pm$ 0.68	16.13	1.056	782 <sup>+30</sup> <sub>-29</sub>	J174750.2-371516
29	113783	-14.14 $\pm$ 1.01	-49.68 $\pm$ 1.31	16.75	1.448	274 <sup>+15</sup> <sub>-14</sub>	J174742.3-364339
29	131780	-51.76 $\pm$ 0.46	-20.30 $\pm$ 0.48	17.23	1.731	170 <sup>+12</sup> <sub>-11</sub>	J174803.3-373208
29	160643	-56.88 $\pm$ 1.41	-14.79 $\pm$ 1.07	16.93	1.459	287 <sup>+17</sup> <sub>-16</sub>	J174753.7-372121
29	168329	-79.27 $\pm$ 0.48	-30.48 $\pm$ 0.53	13.36	1.031	231 <sup>+4</sup> <sub>-4</sub>	J174801.4-371626
29	224715	-55.58 $\pm$ 0.73	28.91 $\pm$ 0.70	17.04	1.223	789 <sup>+45</sup> <sub>-43</sub>	J174804.4-365036
30	152246	-40.60 $\pm$ 0.78	-32.51 $\pm$ 0.86	12.00	1.512	25 <sup>+1</sup> <sub>-1</sub>	J180107.1-283547
30	583187	-102.79 $\pm$ 1.82	-33.05 $\pm$ 1.79	14.32	1.538	66 <sup>+2</sup> <sub>-2</sub>	J180149.2-291502
31	340708	-60.31 $\pm$ 0.69	-29.90 $\pm$ 0.86	13.49	1.395	75 <sup>+2</sup> <sub>-2</sub>	J180208.7-282637
31	562353	-55.37 $\pm$ 1.99	-28.31 $\pm$ 2.42	13.42	1.460	57 <sup>+1</sup> <sub>-1</sub>	J180233.8-281815
31	738841	-72.71 $\pm$ 1.46	-3.25 $\pm$ 1.38	13.84	1.473	66 <sup>+2</sup> <sub>-2</sub>	J180252.7-282247
32	388121	-197.37 $\pm$ 6.71	-21.23 $\pm$ 6.83	14.68	1.225	264 <sup>+7</sup> <sub>-7</sub>	J180311.7-281322
32	397369	-186.58 $\pm$ 9.32	-15.52 $\pm$ 9.63	14.68	1.225	264 <sup>+7</sup> <sub>-7</sub>	J180311.7-281322
32	555529	-38.92 $\pm$ 0.47	-66.83 $\pm$ 0.50	14.81	1.303	211 <sup>+5</sup> <sub>-5</sub>	J180335.2-282237
32	661943	-85.71 $\pm$ 0.53	11.43 $\pm$ 0.68	15.41	1.436	155 <sup>+5</sup> <sub>-5</sub>	J180348.7-284517
32	737206	-168.55 $\pm$ 0.96	-25.28 $\pm$ 0.86	15.34	1.549	103 <sup>+3</sup> <sub>-3</sub>	J180342.9-282535
33	12568	-86.55 $\pm$ 2.83	-24.00 $\pm$ 3.42	13.94	1.284	152 <sup>+3</sup> <sub>-3</sub>	J180502.1-291644
33	16638	-74.64 $\pm$ 5.78	-9.61 $\pm$ 7.36	13.94	1.284	152 <sup>+3</sup> <sub>-3</sub>	J180502.1-291644
33	84101	-71.53 $\pm$ 4.21	-29.71 $\pm$ 4.06	14.56	1.496	84 <sup>+2</sup> <sub>-2</sub>	J180514.6-285300
33	566200	-36.89 $\pm$ 1.47	-39.76 $\pm$ 1.57	14.59	1.491	87 <sup>+3</sup> <sub>-2</sub>	J180603.1-291758
34	159315	-62.24 $\pm$ 2.77	17.44 $\pm$ 2.77	13.96	1.970	27 <sup>+1</sup> <sub>-1</sub>	J175752.2-285845
34	465798	2.54 $\pm$ 0.60	-53.74 $\pm$ 0.69	12.40	1.457	36 <sup>+1</sup> <sub>-1</sub>	J175803.7-284425
35	55762	-70.98 $\pm$ 4.59	7.69 $\pm$ 5.65	15.12	1.466	122 <sup>+4</sup> <sub>-4</sub>	J180357.0-280925
35	346292	-63.16 $\pm$ 0.85	-17.71 $\pm$ 1.03	13.87	2.592	13 <sup>+1</sup> <sub>-1</sub>	J180417.9-274610
35	415867	-51.94 $\pm$ 0.76	-19.60 $\pm$ 0.74	14.69	1.568	73 <sup>+2</sup> <sub>-2</sub>	J180435.1-281856
35	692986	-48.32 $\pm$ 0.60	-28.52 $\pm$ 0.59	14.86	1.357	173 <sup>+5</sup> <sub>-4</sub>	J180454.4-275157
36	301724	-55.66 $\pm$ 0.47	4.65 $\pm$ 0.49	15.44	1.431	160 <sup>+5</sup> <sub>-5</sub>	J180524.1-280656
36	375399	-67.05 $\pm$ 4.13	-59.15 $\pm$ 5.08	14.17	1.395	103 <sup>+2</sup> <sub>-2</sub>	J180526.4-274741
36	426923	-64.22 $\pm$ 0.83	-8.93 $\pm$ 0.67	14.32	1.301	169 <sup>+4</sup> <sub>-4</sub>	J180520.4-273216
36	454051	-49.36 $\pm$ 0.89	26.61 $\pm$ 0.93	14.80	1.615	69 <sup>+2</sup> <sub>-2</sub>	J180540.6-282143
36	752090	-52.69 $\pm$ 3.10	-38.95 $\pm$ 2.48	14.19	1.681	46 <sup>+1</sup> <sub>-1</sub>	J180547.5-275834
36	808646	-50.57 $\pm$ 2.00	-13.22 $\pm$ 1.99	14.68	1.015	439 <sup>+11</sup> <sub>-10</sub>	J180548.1-274431
37	20539	-35.38 $\pm$ 3.99	-66.97 $\pm$ 3.76	15.63	1.740	80 <sup>+5</sup> <sub>-4</sub>	J175202.3-301714
37	213626	-61.06 $\pm$ 0.46	-42.74 $\pm$ 0.55	14.36	1.359	136 <sup>+5</sup> <sub>-5</sub>	J175223.7-300659
37	341121	-34.01 $\pm$ 2.31	-42.87 $\pm$ 2.35	14.06	1.898	31 <sup>+1</sup> <sub>-1</sub>	J175233.7-302209
37	441811	-65.04 $\pm$ 0.42	-4.30 $\pm$ 0.42	13.65	1.711	34 <sup>+1</sup> <sub>-1</sub>	J175239.7-294552
37	514546	50.09 $\pm$ 5.04	-21.87 $\pm$ 5.98	14.25	1.974	30 <sup>+1</sup> <sub>-1</sub>	J175249.8-301735
38	190202	-90.13 $\pm$ 0.55	-0.42 $\pm$ 0.55	13.77	1.864	28 <sup>+1</sup> <sub>-1</sub>	J180120.0-302352
38	337622	-72.87 $\pm$ 0.50	-42.35 $\pm$ 0.49	13.21	1.127	171 <sup>+3</sup> <sub>-3</sub>	J180112.8-293900
39	309705	119.30 $\pm$ 4.49	82.80 $\pm$ 2.73	14.87	1.973	40 <sup>+2</sup> <sub>-2</sub>	J175531.5-294638
39	438588	-117.61 $\pm$ 10.98	12.62 $\pm$ 9.67	15.22	1.451	134 <sup>+4</sup> <sub>-4</sub>	J175542.4-300827
39	622098	-80.43 $\pm$ 0.49	-12.58 $\pm$ 0.55	13.35	1.150	174 <sup>+3</sup> <sub>-3</sub>	J175607.9-300852
40	246965	-68.37 $\pm$ 0.57	-3.34 $\pm$ 0.74	15.42	1.269	318 <sup>+9</sup> <sub>-9</sub>	J175051.4-331222
40	258617	-46.64 $\pm$ 1.10	45.75 $\pm$ 1.40	15.86	1.615	112 <sup>+4</sup> <sub>-4</sub>	J175052.6-330943
40	353609	-47.41 $\pm$ 0.59	-32.71 $\pm$ 0.84	15.07	1.511	101 <sup>+3</sup> <sub>-3</sub>	J175110.4-333143
41 <sup>*,†</sup>	47647	-63.59 $\pm$ 5.68	-7.23 $\pm$ 4.80	13.83	1.812	31 <sup>+1</sup> <sub>-1</sub>	J175149.2-331543

Table 3 continued

Field	ID	$\mu_l \pm \sigma_{\mu_l}$ (mas yr <sup>-1</sup> )	$\mu_b \pm \sigma_{\mu_b}$ (mas yr <sup>-1</sup> )	$I$	$I - J$	$d$ (pc)	DENIS-ID
41	353119	-47.07 $\pm$ 0.39	-34.91 $\pm$ 0.41	14.06	2.091	24 <sup>+1</sup> <sub>-1</sub>	J175221.2-331444
41	353277	-63.24 $\pm$ 0.72	-4.09 $\pm$ 0.96	16.30	1.518	175 <sup>+11</sup> <sub>-11</sub>	J175211.8-331614
42	104424	56.34 $\pm$ 0.50	-29.94 $\pm$ 0.54	14.04	1.190	218 <sup>+4</sup> <sub>-3</sub>	J180843.4-264150
42	133638	-507.56 $\pm$ 1.59	18.36 $\pm$ 2.27	11.71	1.294	52 <sup>+1</sup> <sub>-1</sub>	J180847.5-263239
42	365611	-60.24 $\pm$ 0.48	25.42 $\pm$ 0.48	13.83	1.275	150 <sup>+3</sup> <sub>-3</sub>	J180918.2-270123
42	401145	-46.56 $\pm$ 0.85	-58.55 $\pm$ 0.71	15.50	1.621	94 <sup>+3</sup> <sub>-3</sub>	J180906.5-264621
42	551215	-18.23 $\pm$ 0.71	54.02 $\pm$ 0.81	14.24	1.487	75 <sup>+2</sup> <sub>-2</sub>	J180924.0-264338
42	569217	-102.07 $\pm$ 2.93	-31.90 $\pm$ 2.35	13.69	1.201	179 <sup>+3</sup> <sub>-3</sub>	J180930.6-263632
43	116810	-142.32 $\pm$ 0.44	33.05 $\pm$ 0.47	15.08	1.394	158 <sup>+3</sup> <sub>-3</sub>	J173458.9-273835
43	216905	-33.48 $\pm$ 0.90	-45.37 $\pm$ 1.09	15.41	1.915	56 <sup>+2</sup> <sub>-2</sub>	J173500.2-264956
43	217063	-63.00 $\pm$ 0.53	25.12 $\pm$ 0.51	15.76	1.743	85 <sup>+3</sup> <sub>-3</sub>	J173500.4-265038
43	375807	-121.31 $\pm$ 6.73	-51.42 $\pm$ 4.90	15.29	1.925	52 <sup>+2</sup> <sub>-2</sub>	J173539.6-272808
44	270634	-46.52 $\pm$ 1.46	-37.97 $\pm$ 1.70	14.00	3.087	9 <sup>+1</sup> <sub>-1</sub>	J174950.1-300004
45	58948	-52.06 $\pm$ 2.31	-20.00 $\pm$ 2.18	13.74	1.331	116 <sup>+3</sup> <sub>-3</sub>	J180312.2-301131
45	189813	-167.36 $\pm$ 2.54	83.69 $\pm$ 2.02	15.19	1.516	105 <sup>+4</sup> <sub>-4</sub>	J180327.4-302522
45	217690	-51.35 $\pm$ 0.80	-4.72 $\pm$ 0.98	14.69	1.356	160 <sup>+5</sup> <sub>-5</sub>	J180320.2-301439
45	273351	307.88 $\pm$ 21.56	-449.27 $\pm$ 35.34	15.04	1.575	84 <sup>+3</sup> <sub>-3</sub>	J180335.1-295510
45	313160	-110.41 $\pm$ 1.10	-20.94 $\pm$ 1.33	14.02	1.374	108 <sup>+2</sup> <sub>-2</sub>	J180321.8-294338
46*,†	44548	-234.03 $\pm$ 1.40	-65.68 $\pm$ 1.78	14.13	1.643	48 <sup>+1</sup> <sub>-1</sub>	J180408.7-301305
46	188284	-114.48 $\pm$ 1.25	-119.76 $\pm$ 1.19	12.97	1.355	73 <sup>+2</sup> <sub>-2</sub>	J180434.7-301849
46*,†	335077	-120.15 $\pm$ 1.48	-5.47 $\pm$ 1.83	13.63	1.637	38 <sup>+1</sup> <sub>-1</sub>	J180454.0-301436
46	366546	-81.25 $\pm$ 2.00	-31.76 $\pm$ 2.02	14.01	1.362	114 <sup>+3</sup> <sub>-3</sub>	J180445.7-295855
46	419860	-74.00 $\pm$ 8.92	-110.46 $\pm$ 12.58	14.46	1.421	106 <sup>+2</sup> <sub>-2</sub>	J180447.5-293836
47	109894	-53.25 $\pm$ 1.21	-58.63 $\pm$ 1.09	15.11	1.554	92 <sup>+3</sup> <sub>-3</sub>	J172649.5-394908
47	110343	-65.55 $\pm$ 3.37	-70.84 $\pm$ 3.21	15.11	1.554	92 <sup>+3</sup> <sub>-3</sub>	J172649.5-394908
47	137581	-64.92 $\pm$ 0.80	-19.78 $\pm$ 0.94	14.03	1.565	54 <sup>+1</sup> <sub>-1</sub>	J172652.1-392620
47	167716	-91.09 $\pm$ 0.90	-29.39 $\pm$ 1.00	12.27	1.154	105 <sup>+1</sup> <sub>-1</sub>	J172717.7-395915
49	70067	-62.38 $\pm$ 1.63	39.77 $\pm$ 1.69	15.70	1.777	78 <sup>+46</sup> <sub>-29</sub>	J172910.4-404030
49	78098	-52.81 $\pm$ 1.70	-3.73 $\pm$ 2.11	13.50	1.237	148 <sup>+87</sup> <sub>-55</sub>	J172914.3-403248
49	109397	-97.14 $\pm$ 0.80	-70.38 $\pm$ 0.85	13.75	1.147	211 <sup>+124</sup> <sub>-78</sub>	J172919.6-400855
49	113409	-53.78 $\pm$ 0.78	-60.41 $\pm$ 0.88	14.73	1.307	200 <sup>+117</sup> <sub>-74</sub>	J172916.7-400451
49	121079	-129.88 $\pm$ 0.90	-75.05 $\pm$ 1.02	13.71	1.400	81 <sup>+48</sup> <sub>-31</sub>	J172917.6-395552
49	147926	-117.40 $\pm$ 1.60	-22.21 $\pm$ 1.69	14.96	1.527	92 <sup>+54</sup> <sub>-34</sub>	J172943.1-402853
49	161249	-107.87 $\pm$ 0.73	-36.10 $\pm$ 0.76	14.47	1.354	146 <sup>+86</sup> <sub>-54</sub>	J172932.2-401929
49	177184	-37.24 $\pm$ 1.14	-63.34 $\pm$ 1.16	17.25	1.274	725 <sup>+425</sup> <sub>-268</sub>	J172934.8-400434
49	180561	-55.53 $\pm$ 0.78	-10.61 $\pm$ 0.90	16.36	1.627	138 <sup>+81</sup> <sub>-51</sub>	J172934.5-400033

**Table 4.** Nearby ( $d < 50$  pc) OGLE-II high proper motion stars cross-identified with entries in the 2MASS catalogue. Stars are characterized as M-dwarfs based on DENIS  $I - J$  colour. The distance estimate,  $d$ , is determined using the theoretical luminosity model of Baraffe et al. (1998). Error values are derived from random photometric errors, statistical colour-luminosity scatter and systematic offset of the theoretical luminosity model, see text.  $\Delta\theta$  and  $\Delta\phi$  are the differences in star position between the OGLE-II and DENIS catalogues and the DENIS and 2MASS catalogues respectively. See Section 7 for an explanation of the star and dagger symbols in column 1.

UID	OGLE-II		DENIS	2MASS	$\Delta\theta$	$\Delta\phi$	DENIS photometry			2MASS photometry		$d$
	Field	ID	ID	ID	(as)	(as)	$I$	$J$	$K_s$	$J$	$K_s$	(pc)
1	1	238184	J180222.9-301005	18022356-3010044	3.48	8.031	15.163	13.247 $\pm$ 0.13		7.679 $\pm$ 0.02	6.053 $\pm$ 0.03	50 $^{+38}_{-22}$
2	1	701357	J180259.7-293831	18025972-2938310	3.04	0.554	13.480	11.925 $\pm$ 0.25	10.803 $\pm$ 0.15	11.604 $\pm$ 0.02	10.486 $\pm$ 0.02	43 $^{+33}_{-19}$
3	2	426502	J180429.7-291729	18042976-2917298	3.35	0.403	12.915	11.157 $\pm$ 0.08	9.927 $\pm$ 0.11	11.184 $\pm$ 0.03	9.951 $\pm$ 0.03	22 $^{+17}_{-10}$
4	3	64760	J175301.9-300832	17530194-3008328	3.65	0.327	15.087	13.090 $\pm$ 0.08		13.441 $\pm$ 0.07	12.272 $\pm$ 0.06	43 $^{+33}_{-19}$
5	3	216180	J175330.8-302535	17533087-3025354	3.22	0.347	13.383	11.130 $\pm$ 0.06	9.474 $\pm$ 0.07	11.060 $\pm$ 0.03	9.538 $\pm$ 0.03	15 $^{+11}_{-6}$
6	3	229801	J175327.9-301913	17532796-3019138	3.18	0.422	13.653	11.597 $\pm$ 0.06	10.260 $\pm$ 0.07	11.640 $\pm$ 0.02	10.284 $\pm$ 0.03	21 $^{+16}_{-9}$
7*	3	370016	J175329.3-294140	17532930-2941398	0.78	0.887	13.830	11.996 $\pm$ 0.07		11.822 $\pm$	11.271 $\pm$ 0.09	30 $^{+23}_{-13}$
8	4	231890	J175431.3-300158	17543132-3001585	2.10	0.313	14.393	12.564 $\pm$ 0.08	11.378 $\pm$ 0.08	12.776 $\pm$ 0.06	11.431 $\pm$ 0.04	40 $^{+30}_{-17}$
9*	4	254212	J175429.1-295718	17542912-2957184	0.65	0.342	11.887	10.379 $\pm$ 0.06	9.377 $\pm$ 0.05	10.624 $\pm$ 0.04	9.479 $\pm$ 0.03	24 $^{+18}_{-10}$
10	4	614523	J175454.4-300223	17545444-3002239	2.66	0.445	13.426	11.449 $\pm$ 0.06	10.164 $\pm$ 0.07	11.494 $\pm$ 0.04	10.186 $\pm$ 0.04	21 $^{+16}_{-9}$
11	4	625701	J175457.0-300005	17545702-3000061	3.81	0.762	14.892	12.854 $\pm$ 0.09	11.729 $\pm$ 0.09	12.865 $\pm$	11.537 $\pm$	37 $^{+28}_{-16}$
12	4	734288	J175503.6-292621	17550366-2926218	1.43	0.362	15.038	12.369 $\pm$ 0.07	11.060 $\pm$ 0.09	12.391 $\pm$ 0.05	11.038 $\pm$ 0.05	21 $^{+16}_{-9}$
13	5	38999	J174950.1-300004	17495008-3000044	3.01	0.887	14.002	10.915 $\pm$ 0.07	8.811 $\pm$ 0.06	10.792 $\pm$ 0.03	8.693 $\pm$ 0.03	9 $^{+7}_{-4}$
14	5	208658	J175027.5-301923	17502760-3019239	2.66	0.822	14.014	11.362 $\pm$ 0.08	9.558 $\pm$ 0.08	11.356 $\pm$ 0.04	9.661 $\pm$ 0.03	13 $^{+11}_{-6}$
15	5	244353	J175036.2-300145	17503622-3001454	1.95	0.286	16.076	13.353 $\pm$ 0.11		13.427 $\pm$ 0.08	12.044 $\pm$ 0.06	32 $^{+25}_{-14}$
16*,†	8	98776	J182247.8-212100	18224781-2121005	0.40	0.480	13.796	11.684 $\pm$ 0.09	10.342 $\pm$ 0.08	11.612 $\pm$ 0.03	10.283 $\pm$ 0.03	21 $^{+16}_{-9}$
17	8	350020	J182326.3-214906	18232632-2149060	2.54	0.512	13.677	12.112 $\pm$ 0.08	11.064 $\pm$ 0.07	12.167 $\pm$ 0.02	11.114 $\pm$ 0.02	46 $^{+35}_{-20}$
18	12	51118	J181541.4-240408	18154140-2404093	3.33	1.051	13.115	11.264 $\pm$ 0.07	9.923 $\pm$ 0.06	11.319 $\pm$ 0.02	9.962 $\pm$ 0.03	21 $^{+17}_{-9}$
19*,†	14	525442	J174719.4-231412	17471940-2314118	0.79	0.881	15.656	13.349 $\pm$ 0.10	12.633 $\pm$ 0.14	13.451 $\pm$ 0.07	12.438 $\pm$ 0.06	40 $^{+30}_{-17}$
20	15	521758	J174832.0-230851	17483208-2308508	3.36	0.757	13.986	12.339 $\pm$ 0.08		12.428 $\pm$ 0.06	11.344 $\pm$ 0.06	44 $^{+34}_{-20}$
21	19	258847	J180753.1-272126	18075311-2721268	3.76	0.580	14.560	12.341 $\pm$ 0.11	10.919 $\pm$ 0.08	12.344 $\pm$ 0.03	10.891 $\pm$ 0.02	26 $^{+20}_{-11}$
22	20	445532	J175934.3-291030	17593434-2910305	2.06	0.038	13.525	11.750 $\pm$ 0.10	10.537 $\pm$ 0.09	11.764 $\pm$ 0.03	10.534 $\pm$ 0.03	29 $^{+22}_{-12}$
23	20	596512	J175949.8-291926	17594987-2919257	3.55	0.800	13.676	11.143 $\pm$ 0.09	9.806 $\pm$ 0.09	11.224 $\pm$ 0.04	9.725 $\pm$ 0.03	13 $^{+10}_{-5}$
24	21	140	J175949.8-291926	17594987-2919257	3.53	0.800	13.676	11.143 $\pm$ 0.09	9.806 $\pm$ 0.09	11.224 $\pm$ 0.04	9.725 $\pm$ 0.03	13 $^{+10}_{-5}$
25	21	649329	J180023.9-282744	18002390-2827450	3.04	0.860	13.414	11.794 $\pm$ 0.10	10.457 $\pm$ 0.09	11.797 $\pm$ 0.04	10.551 $\pm$ 0.04	36 $^{+28}_{-16}$
26	22	681768	J175705.2-303146	17570526-3031455	3.33	0.949	15.246	13.263 $\pm$ 0.10	12.054 $\pm$ 0.11	13.522 $\pm$ 0.08	12.147 $\pm$ 0.06	47 $^{+36}_{-21}$
27	23	281219	J175740.8-311443	17574089-3114437	1.55	0.614	14.736	12.939 $\pm$ 0.08	11.469 $\pm$ 0.08	12.759 $\pm$ 0.03	11.445 $\pm$ 0.02	49 $^{+37}_{-21}$
28	25	327263	J175441.4-331626	17544144-3316268	3.72	0.377	13.145	9.841 $\pm$ 0.05	8.183 $\pm$ 0.04	9.860 $\pm$ 0.02	8.221 $\pm$ 0.02	5 $^{+4}_{-2}$
29*,†	25	592433	J175443.1-323213	17544314-3232134	0.61	0.044	12.052	10.580 $\pm$ 0.06	9.712 $\pm$ 0.06	10.626 $\pm$ 0.03	9.768 $\pm$ 0.02	29 $^{+22}_{-13}$
30	30	152246	J180107.1-283547	18010706-2835458	1.86	1.947	11.998	10.486 $\pm$ 0.06	9.571 $\pm$ 0.07	10.410 $\pm$ 0.02	9.546 $\pm$ 0.03	25 $^{+19}_{-11}$
31	34	159315	J175752.2-285845	17575241-2858464	1.90	2.373	13.960	11.990 $\pm$ 0.08		12.170 $\pm$ 0.04	11.068 $\pm$ 0.04	27 $^{+20}_{-11}$
32	34	465798	J175803.7-284425	17580385-2844256	1.72	1.397	12.405	10.948 $\pm$ 0.06	10.183 $\pm$ 0.06	11.009 $\pm$ 0.03	10.218 $\pm$ 0.03	36 $^{+27}_{-16}$
33	35	346292	J180417.9-274610	18041796-2746096	2.94	0.888	13.873	11.281 $\pm$ 0.07		11.364 $\pm$ 0.02	9.880 $\pm$ 0.02	13 $^{+10}_{-5}$
34	36	752090	J180547.5-275834	18054752-2758351	1.14	0.735	14.186	12.505 $\pm$ 0.08	11.279 $\pm$ 0.08	12.545 $\pm$ 0.06	11.356 $\pm$ 0.04	46 $^{+35}_{-20}$
35	37	341121	J175233.7-302209	17523369-3022098	1.14	0.754	14.061	12.163 $\pm$ 0.11	10.943 $\pm$ 0.10	12.117 $\pm$ 0.03	10.946 $\pm$ 0.03	31 $^{+24}_{-13}$
36	37	441811	J175239.7-294552	17523977-2945521	3.19	0.499	13.655	11.944 $\pm$ 0.07	10.701 $\pm$ 0.07	12.061 $\pm$ 0.06	10.797 $\pm$ 0.05	34 $^{+26}_{-15}$
37	37	514546	J175249.8-301735	17524989-3017358	2.97	0.655	14.247	12.273 $\pm$ 0.07	10.958 $\pm$ 0.07	12.247 $\pm$ 0.05	10.918 $\pm$ 0.04	30 $^{+23}_{-13}$
38	38	190202	J180120.0-302352	18012009-3023526	2.74	0.643	13.770	11.906 $\pm$ 0.06	10.488 $\pm$ 0.07	11.894 $\pm$ 0.04	10.570 $\pm$ 0.03	28 $^{+22}_{-12}$
39	39	309705	J175531.5-294638	17553162-2946396	0.40	1.548	14.874	12.901 $\pm$ 0.08	11.548 $\pm$ 0.10	12.150 $\pm$	10.809 $\pm$	40 $^{+31}_{-18}$
40*,†	41	47647	J175149.2-331543	17514924-3315428	0.47	0.616	13.830	12.018 $\pm$ 0.06	10.650 $\pm$ 0.07	12.027 $\pm$ 0.03	10.729 $\pm$ 0.02	31 $^{+24}_{-14}$
41	41	353119	J175221.2-331444	17522121-3314439	3.58	0.727	14.063	11.972 $\pm$ 0.11	10.714 $\pm$ 0.10	11.990 $\pm$ 0.05	10.554 $\pm$	24 $^{+18}_{-10}$
42	44	270634	J174950.1-300004	17495008-3000044	3.01	0.887	14.002	10.915 $\pm$ 0.07	8.811 $\pm$ 0.06	10.792 $\pm$ 0.03	8.693 $\pm$ 0.03	9 $^{+7}_{-4}$
43*,†	46	44548	J180408.7-301305	18040875-3013055	0.62	0.101	14.128	12.485 $\pm$ 0.08	11.577 $\pm$ 0.13	12.480 $\pm$ 0.02	11.596 $\pm$ 0.02	48 $^{+36}_{-21}$
44*,†	46	335077	J180454.0-301436	18045398-3014368	0.69	0.897	13.634	11.997 $\pm$ 0.09	10.983 $\pm$ 0.11	12.090 $\pm$ 0.04	11.023 $\pm$ 0.03	38 $^{+29}_{-17}$

## REFERENCES

- Alcock, C., Allsman, R.A., Alves, D.R., Axelrod, T.S., Becker, A.C., Bennett, D.P., Cook, K.H., Drake, A.J., et al., 2000, *ApJ*, 541, 734
- Alcock, C., Allsman, R.A., Alves, D.R., Axelrod, T.S., Becker, A.C., Bennett, D.P., Cook, K.H., Drake, A.J., et al., 2001, *ApJ*, 562, 337
- Aubourg, E., Bareyre, P., Brehin, S., Gros, M., Lachieze-Rey, M., Laurent, B., Lesquoy, E., Magneville, C., et al., 1993, *Nature*, 365, 623
- Baraffe, I., Chabrier, G., Allard, F., Hauschildt, P.H., 1998, *A&A*, 337, 403
- Bergeron, P., Wesemael, F., Beauchamp, A., 1995, *PASP*, 107, 1047
- Bond, I.A., Abe, F., Dodd, R.J., Hearnshaw, J.B., Honda, M., Jugaku, J., Kilmartin, P.M., Marles, A., et al., 2001, *MNRAS*, 327, 868
- Carpenter, J.M., 2001, *AJ*, 121, 2851
- Cutri, R.M., Skrutskie, M.F., van Dyk, S., Beichman, C.A., Carpenter, J.M., Chester, T., Cambresy, L., Evans, T., et al., 2003, 2MASS All Sky Catalog of point sources., The IRSA 2MASS All-Sky Point Source Catalog, NASA/IPAC Infrared Science Archive. <http://irsa.ipac.caltech.edu/applications/Gator/>
- Cutri, R.M., Skrutskie, M.F., van Dyk, S., Beichman, C.A., Carpenter, J.M., Chester, T., Cambresy, L., Evans, T., et al., 2005, Explanatory Supplement to the 2MASS All Sky Data Release and Extended Mission Products, Technical report, Caltech, <http://www.ipac.caltech.edu/2mass/releases/allsky/doc-explsup.html>
- Dahn, C.C., Harris, H.C., Vrba, F.J., Guetter, H.H., Canzian, B., Henden, A.A., Levine, S.E., Luginbuhl, C.B., et al., 2002, *AJ*, 124, 1170
- Edvardsson, B., Andersen, J., Gustafsson, B., Lambert, D.L., Nissen, P.E., Tomkin, J., 1993, *A&A*, 275, 101
- Epchtein, N., de Batz, B., Capolani, L., Chevallier, L., Copet, E., Fouque, P., Lacombe, F., Le Bertre, T., et al., 1997, *The Messenger*, 87, 27
- Eyer, L., Woźniak, P.R., 2001, *MNRAS*, 327, 601
- Gliese, W., Jahreiß, H., 1991, Preliminary Version of the Third Catalogue of Nearby Stars, Technical report
- Henry, T.J., Ianna, P.A., Kirkpatrick, J.D., Jahreiss, H., 1997, *AJ*, 114, 388
- Hoeg, E., Bässgen, G., Bastian, U., Egret, D., Fabricius, C., Großmann, V., Halbwachs, J.L., Makarov, V.V., et al., 1997, *A&A*, 323, L57
- Ibukiyama, A., Arimoto, N., 2002, *A&A*, 394, 927
- Landolt, A.U., 1992, *AJ*, 104, 372
- Lejeune, T., Cuisinier, F., Buser, R., 1997, *A&AS*, 125, 229
- Mao, S., Paczyński, B., 2002, *MNRAS*, 337, 895
- Perryman, M.A.C., ESA, editors, 1997, The HIPPARCOS and TYCHO catalogues. Astrometric and photometric star catalogues derived from the ESA HIPPARCOS Space Astrometry Mission, volume 1200 of ESA Special Publication
- Perryman, M.A.C., Lindegren, L., Kovalevsky, J., Hoeg, E., Bastian, U., Bernacca, P.L., Crézé, M., Donati, F., et al., 1997, *A&A*, 323, L49
- Phan-Bao, N., Guibert, J., Crifo, F., Delfosse, X., Forveille, T., Borsenberger, J., Epchtein, N., Fouqué, P., et al., 2001, *A&A*, 380, 590
- Rattenbury, N.J., Mao, S., Debattista, V.P., Sumi, T., Gerhard, O., de Lorenzi, F., 2007a, *MNRAS*, 378, 1165
- Rattenbury, N.J., Mao, S., Sumi, T., Smith, M.C., 2007b, *MNRAS*, 378, 1064
- Reid, I.N., Cruz, K.L., Laurie, S.P., Liebert, J., Dahn, C.C., Harris, H.C., Guetter, H.H., Stone, R.C., et al., 2003, *AJ*, 125, 354
- Reylé, C., Robin, A.C., 2004, *A&A*, 421, 643
- Reylé, C., Robin, A.C., Scholz, R.D., Irwin, M., 2002, *A&A*, 390, 491
- Robin, A.C., Reylé, C., Derrière, S., Picaud, S., 2003, *A&A*, 409, 523
- Soszynski, I., Zebrun, K., Udalski, A., Wozniak, P.R., Szymanski, M., Kubiak, M., Pietrzynski, G., Szewczyk, O., et al., 2002, *Acta Astronomica*, 52, 143
- Sumi, T., Abe, F., Bond, I.A., Dodd, R.J., Hearnshaw, J.B., Honda, M., Honma, M., Kan-ya, Y., et al., 2003a, *ApJ*, 591, 204
- Sumi, T., Eyer, L., Woźniak, P.R., 2003b, *MNRAS*, 340, 1346
- Sumi, T., Wu, X., Udalski, A., Szymański, M., Kubiak, M., Pietrzyński, G., Soszyński, I., Woźniak, P., et al., 2004, *MNRAS*, 348, 1439
- The Denis Consortium, 2005, VizieR Online Data Catalog, 1, 2002
- Udalski, A., Kubiak, M., Szymanski, M., 1997, *Acta Astronomica*, 47, 319
- Udalski, A., Szymanski, M., Kubiak, M., Pietrzynski, G., Soszynski, I., Wozniak, P., Zebrun, K., Szewczyk, O., et al., 2002, *Acta Astronomica*, 52, 217
- Udalski, A., Zebrun, K., Szymanski, M., Kubiak, M., Pietrzynski, G., Soszynski, I., Wozniak, P., 2000, *Acta Astronomica*, 50, 1
- Woolley, R.v.d.R., 1970, *Royal Observatory Annals*, 5